Nucleon Electromagnetic Form Factors and Densities

James J. Kelly

University of Maryland

Motivation: What does it look like?

- Electromagnetic form factors test fundamental properties.
- Much recent effort to improve precision and Q^2 range, corresponding to better spatial resolution.
- Recent discovery that G_{Ep}/G_{Mp} falls suggests more diffuse charge, but how much?
- Form factors calculable directly, but intuition stronger in space than momentum.

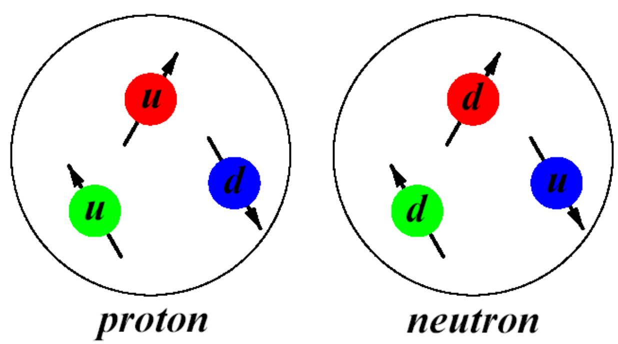

Outline

- Introduction
- Brief review of unpolarized data
- Recent data from polarization techniques
- Comparison with representative models
- Parametrization of intrinsic form factor
- Extraction of radial densities
  - relativistic inversion method
  - survey of results
  - discrete ambiguities
- Conclusions
- Future prospects

Sachs Form Factors

Matrix elements of the nucleon e.m. current

$$\Gamma^{\mu} = F_1(Q^2) + \kappa F_2(Q^2)\frac{i\sigma^{\mu\nu}q_{\nu}}{2m}$$

appear simplest in the Breit frame

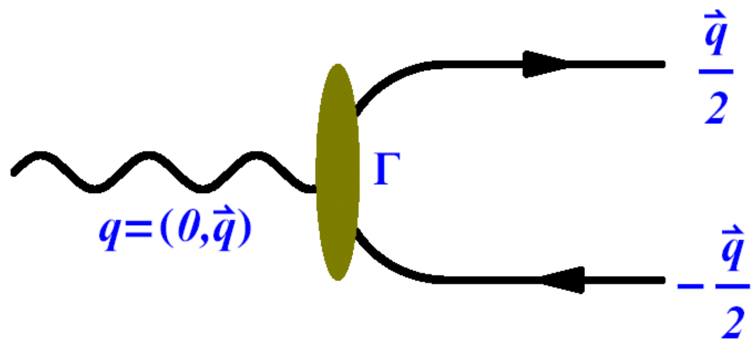

$$\bar{u}(p',s')\Gamma^{\mu}u(p,s) = \chi^{*}_{s'}\left(G_E + \frac{i\vec{\sigma}\times\vec{q}}{2m}G_M\right)\chi_s$$

where charge and current contributions are represented by Sachs form factors:

$$G_E = F_1 - \tau\kappa F_2$$
$$G_M = F_1 + \kappa F_2$$

Rosenbluth Separation

$$\frac{\varepsilon(1+\tau)}{\sigma_{NS}}\frac{d\sigma}{d\Omega} = \tau\, G_M^2 + \varepsilon\, G_E^2$$

- Intercept and slope give G_M and G_E.
- G_M dominates for large τ.
- Must control kinematics, acceptances, and radiative corrections very accurately because coefficient is strong function of angle.

Rosenbluth data consistent with 1-photon exchange.

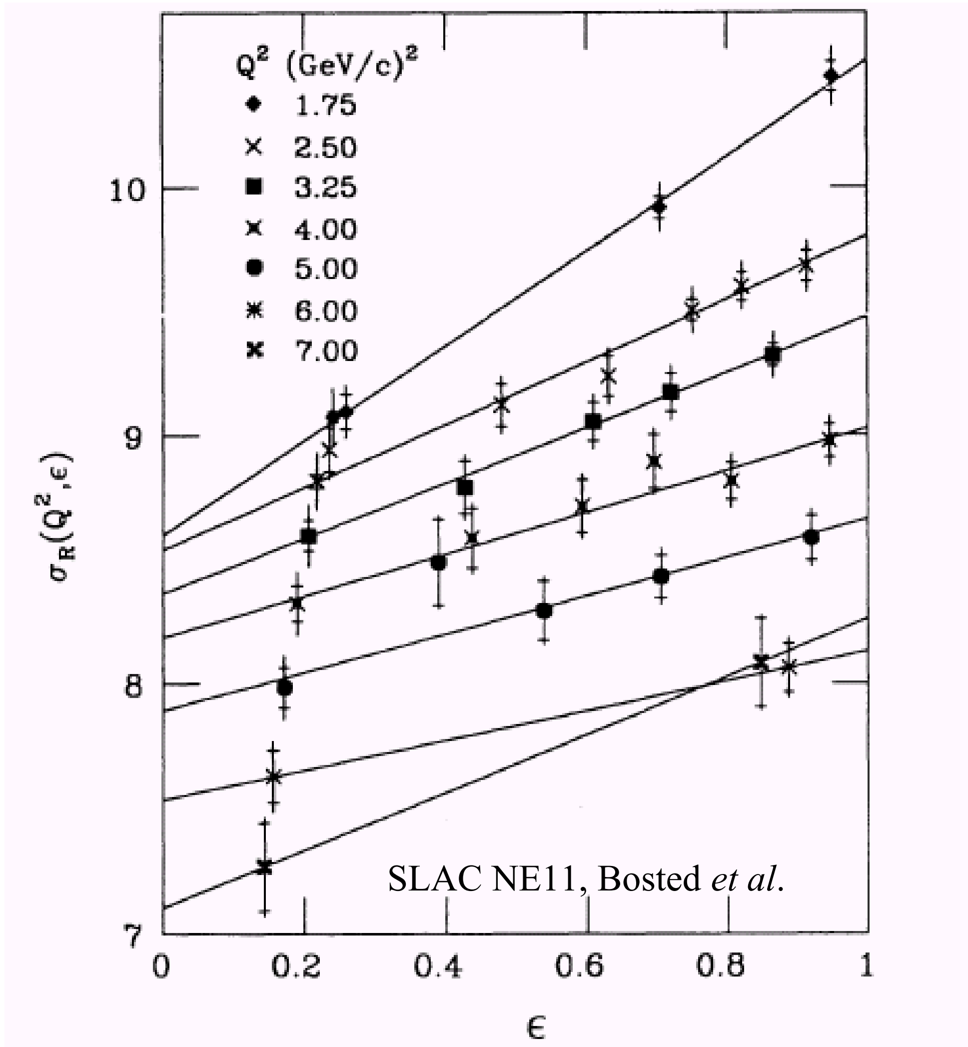

Proton Form Factors from Rosenbluth

- G_{Ep} consistent with G_D, but
  - uncertainties relatively large for Q^2>1
  - systematic differences may show Rosenbluth limitations
  - VMD+pQCD fits depend upon data selection
- G_{Mp} clearly modified wrt G_D at large Q^2

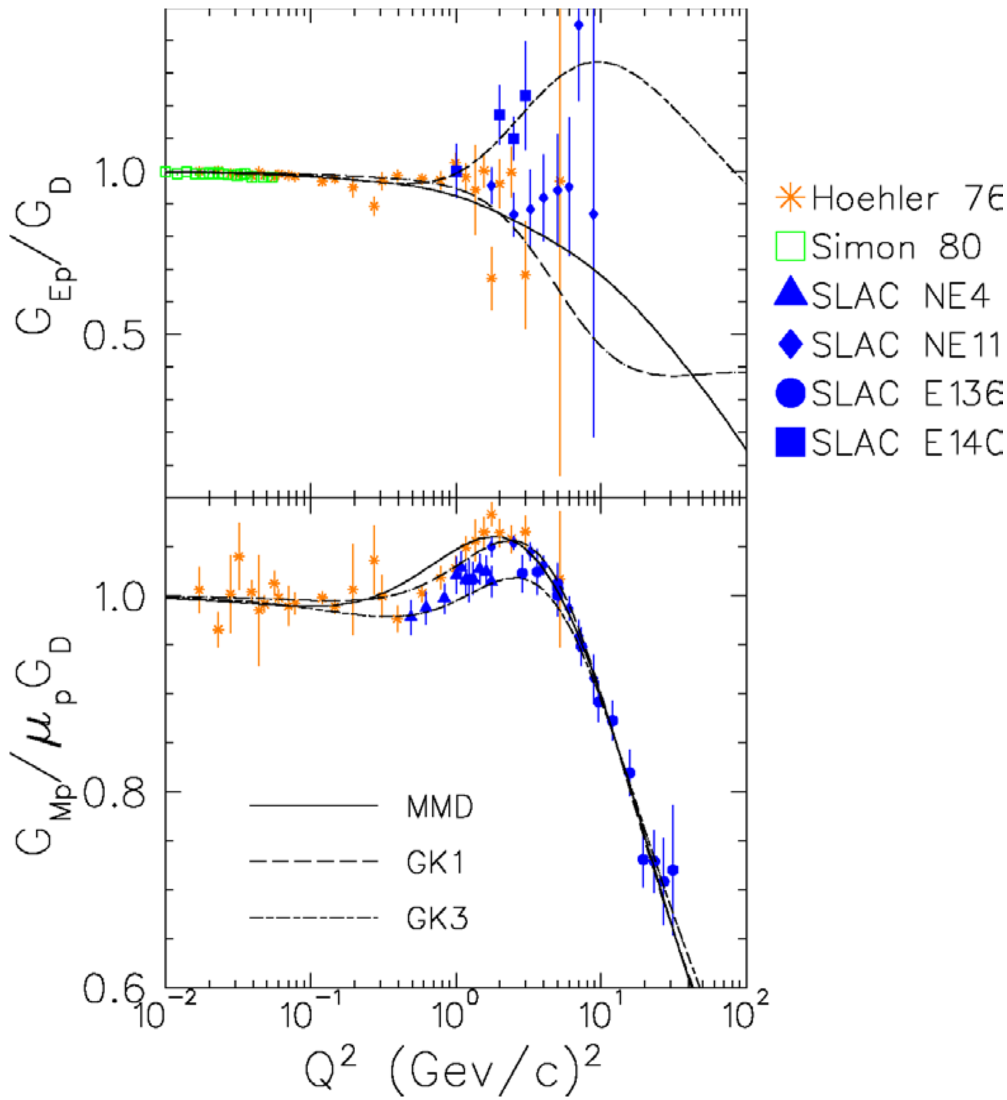

Unpolarized Neutron Data

- G_{En} limited to low Q^2
- G_{Mn} at high Q^2 from inclusive cross section clearly drops wrt G_D
- G_{Mn} at low Q^2 from
  - d(e,e'n) with efficiency by associated particle
  - d(e,e'n)/d(e,e'p) with kinematically complete efficiency (red)
  - Systematic differences as large as deviation from G_D

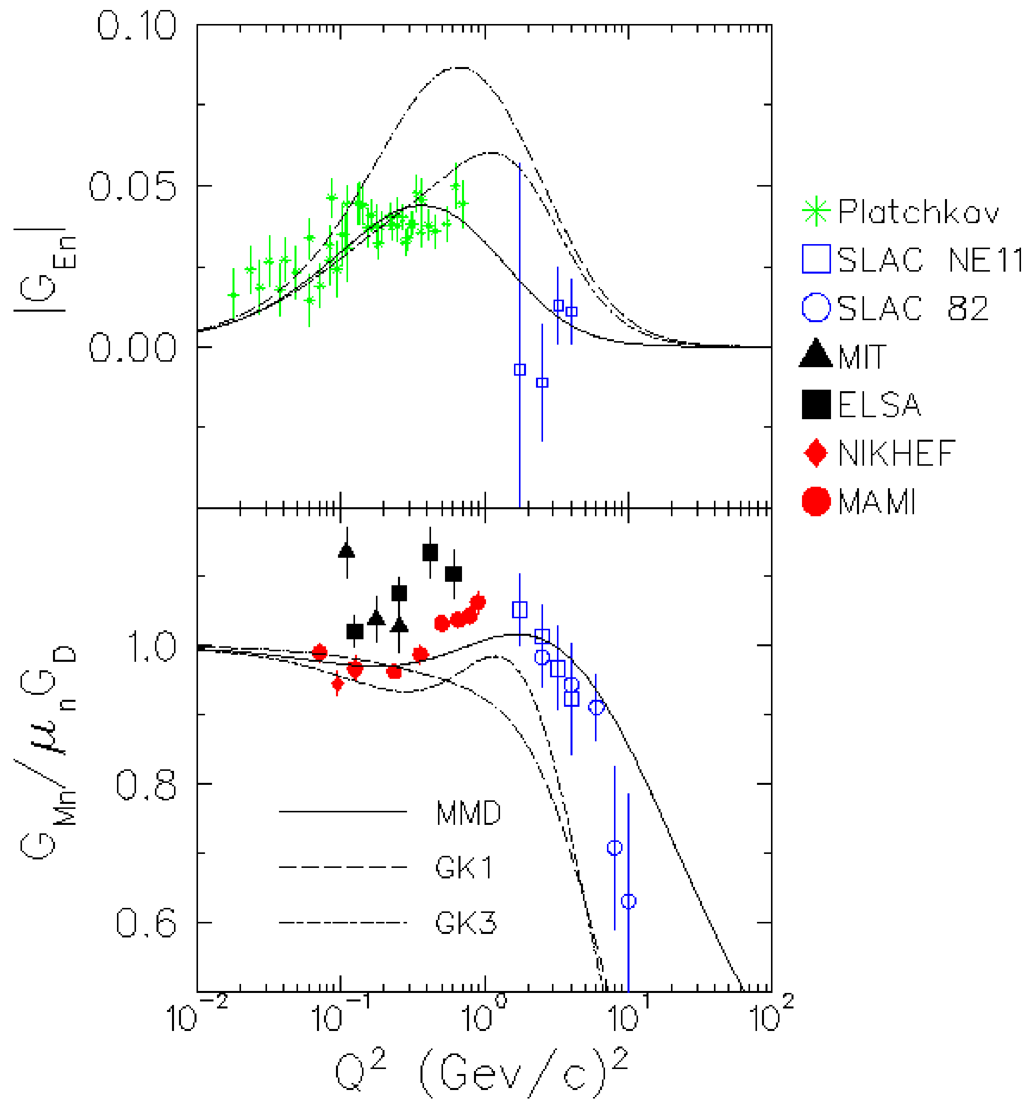

Model dependence G_{En} from d(e,e)d

- Corrections:
  - Proton contribution
  - G_{Mn} contribution
  - Target structure
  - MEC+IC
- Each model shown gives equivalent fit to deuteron elastic scattering
- Usually quote Paris, but model dependence ~50%

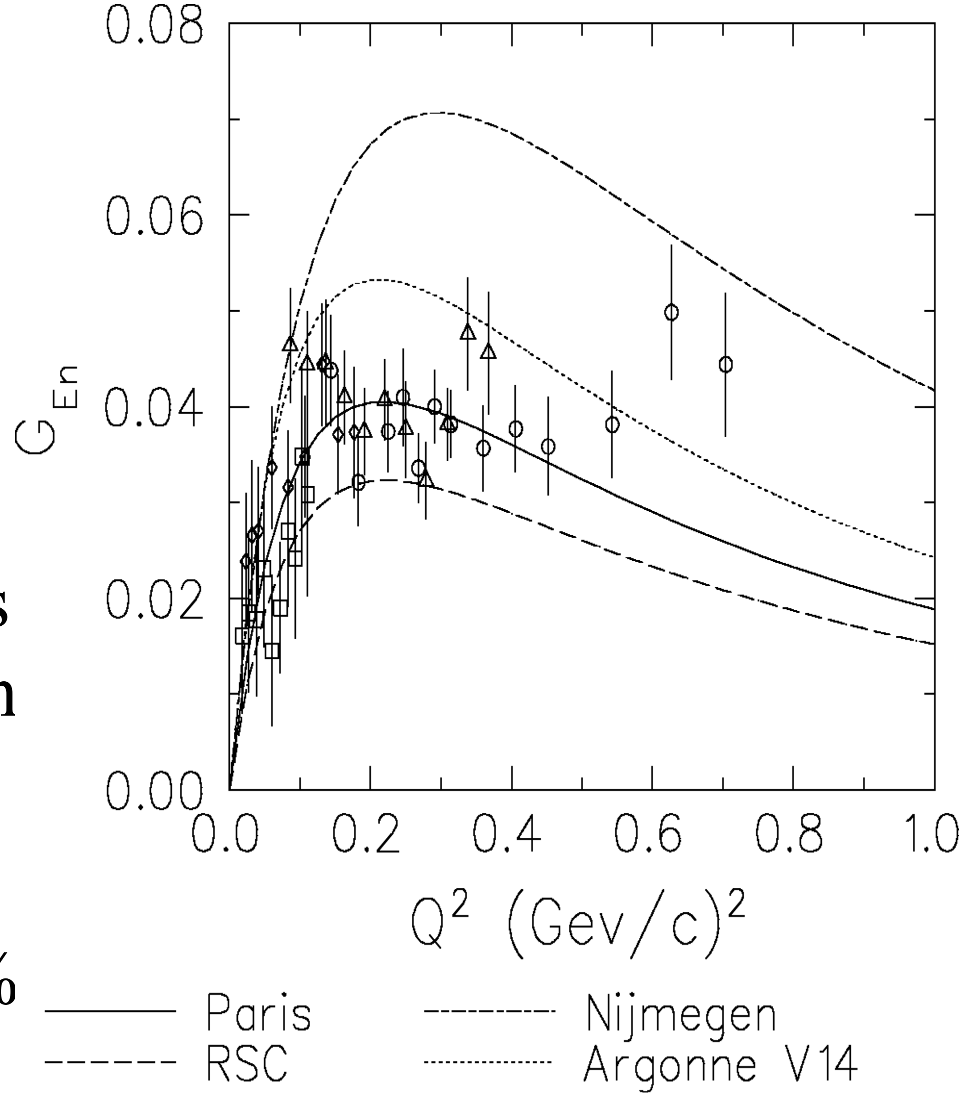

Recoil Polarization

$$\frac{d\sigma}{dp_N d\Omega_N d\Omega_e} = \overline{\sigma}\left(1 + \vec{S}\cdot\vec{P} + h(A + \vec{S}\cdot\vec{P}')\right)$$

$$quasifree \Rightarrow \frac{P'_S}{P'_L} = -\sqrt{\frac{2\varepsilon}{\tau(1+\varepsilon)}}\frac{G_E}{G_M}$$

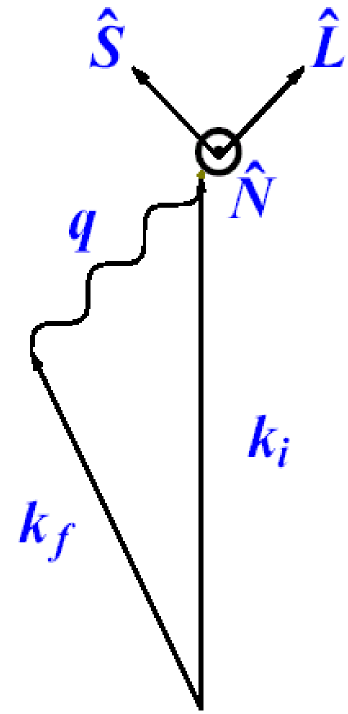

- Polarization ratio linear in G_E, sensitive to sign.
- Minimizes systematic uncertainties due to acceptance and kinematic variations.
- Simultaneous measurement of components minimizes systematic uncertainties due to beam polarization and analyzing power.
- Dominant systematic uncertainty due to spin precession.

G_{Ep}/G_{Mp} by Recoil Polarization

JLab E93-027, Perdrisat *et al*.

- Phase shift in azimuthal distribution proportional to G_{Ep}/G_{Mp}.
- Dashed curve assumes $G_{Ep}=G_D$. Reduced phase shift demonstrates reduced G_{Ep}.

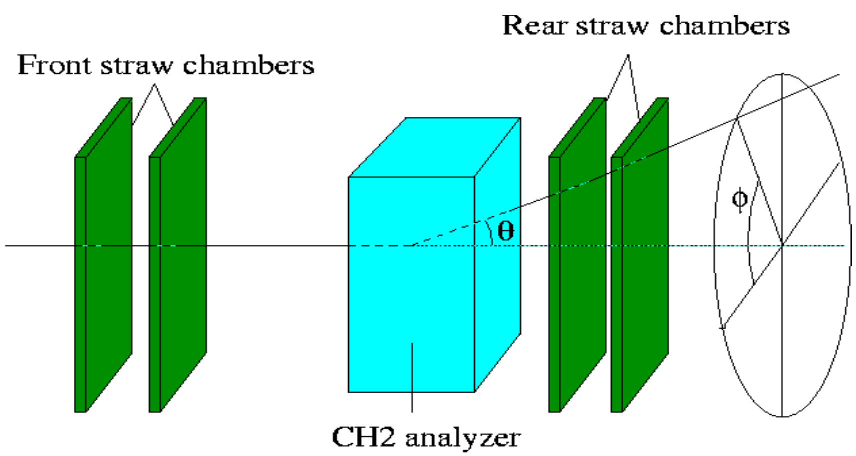

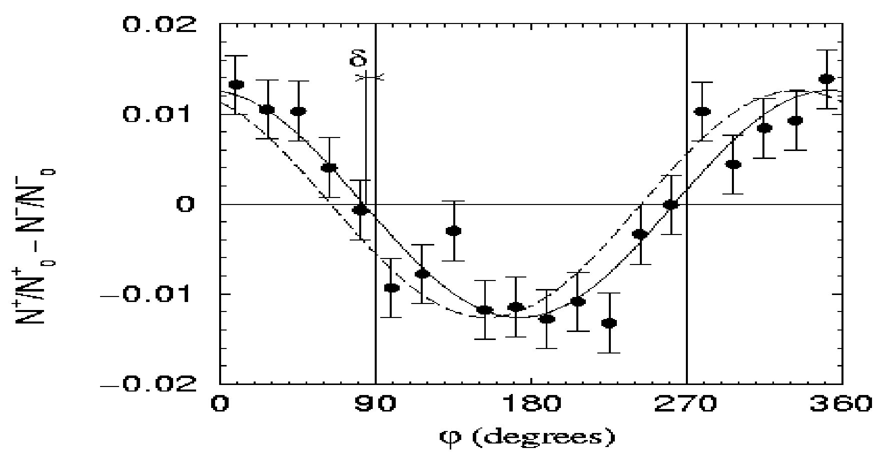

Proton Electromagnetic Ratio

- Average Rosenbluth data near unity, but scatter fairly large for $Q^2>1$.
- New recoil polarization data:
  - show strong linear decrease for $Q^2>1$
  - suggest charge broader than magnetization
- New "super Rosenbluth" experiment should provide independent check.

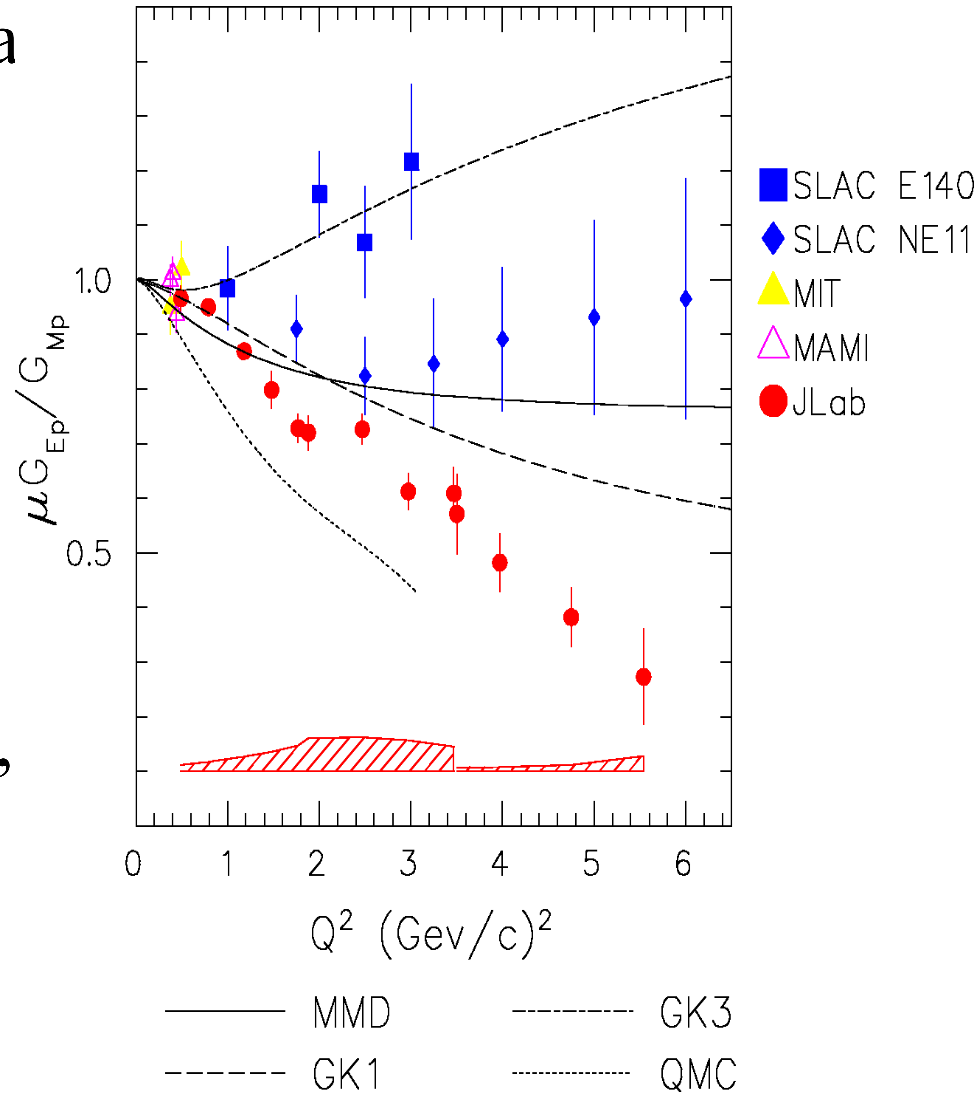

Quasifree Recoil Polarization

- Recoil polarization for quasifree *d(e,e´N)* relatively insensitive to Fermi motion, FSI, MEC+IC.
- Acceptance averaging and nuclear corrections of order few % for $Q^2>0.5$.

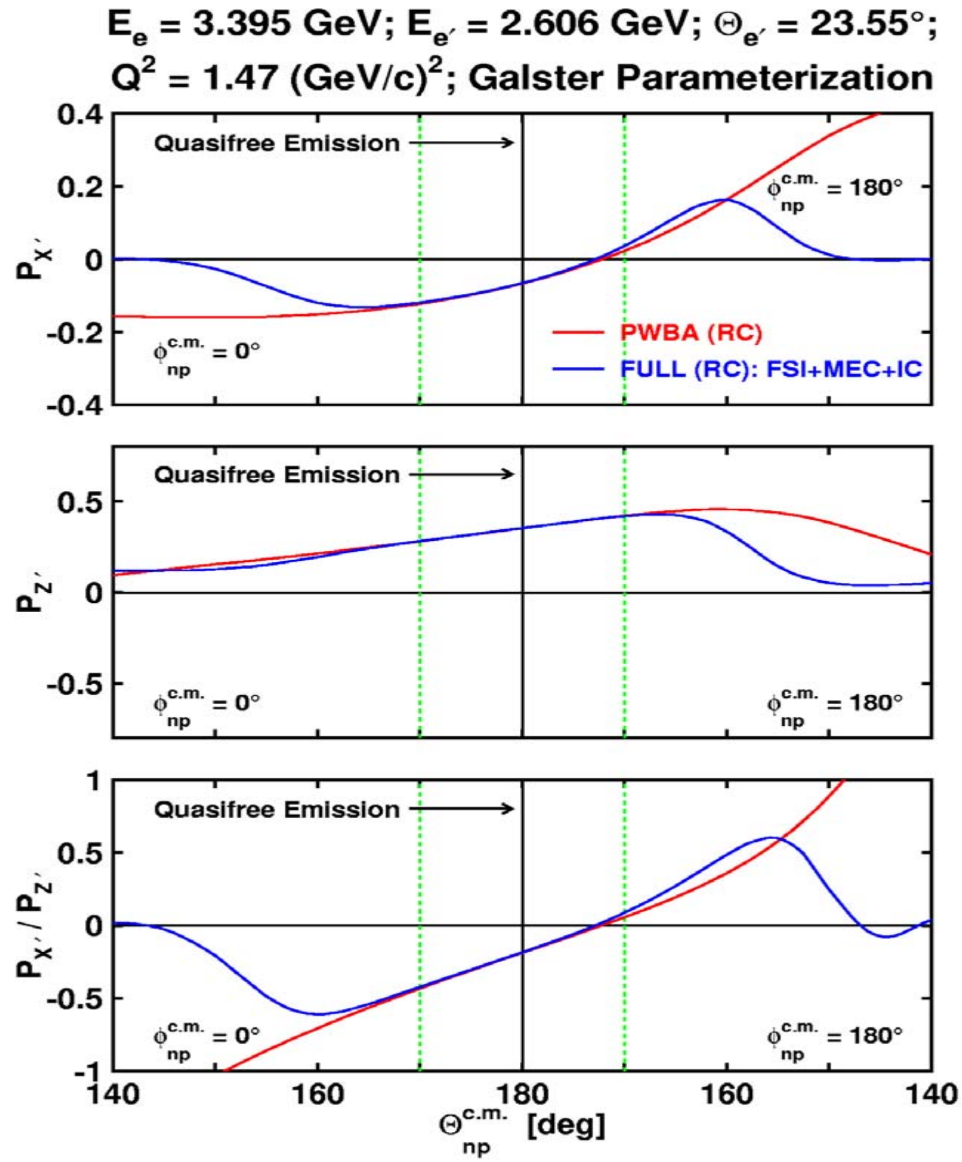

Neutron Recoil Polarization at JLab

E93-038, Madey *et al.*

- Dipole magnet for spin precession
- Lead curtain suppresses background
- Front tagger identifies charged particles
- 4x5 front array detects nucleon
- Rear tagger distinguishes (n,n) from (n,p)
- Segmentation permits tracking
- Up/down asymmetry measures sideways polarization

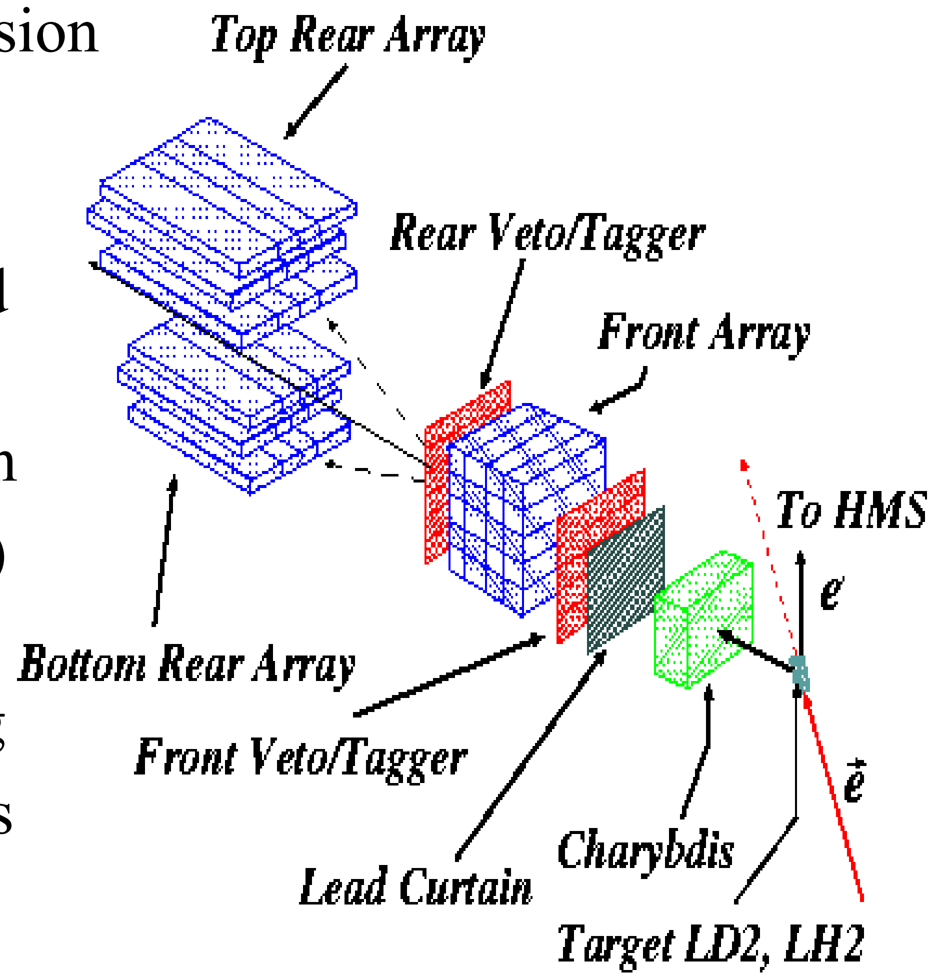

Neutron Time Spectra

- Careful alignment of mean times using simple events
- Position from time differences
- Compare measured-predicted times using electron kinematics and nucleon angles.
- Obtain good signal/noise

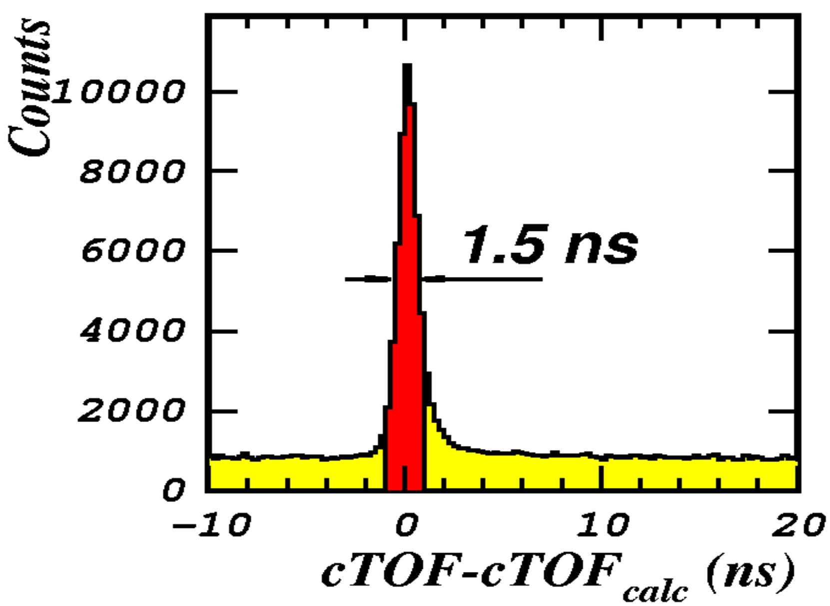

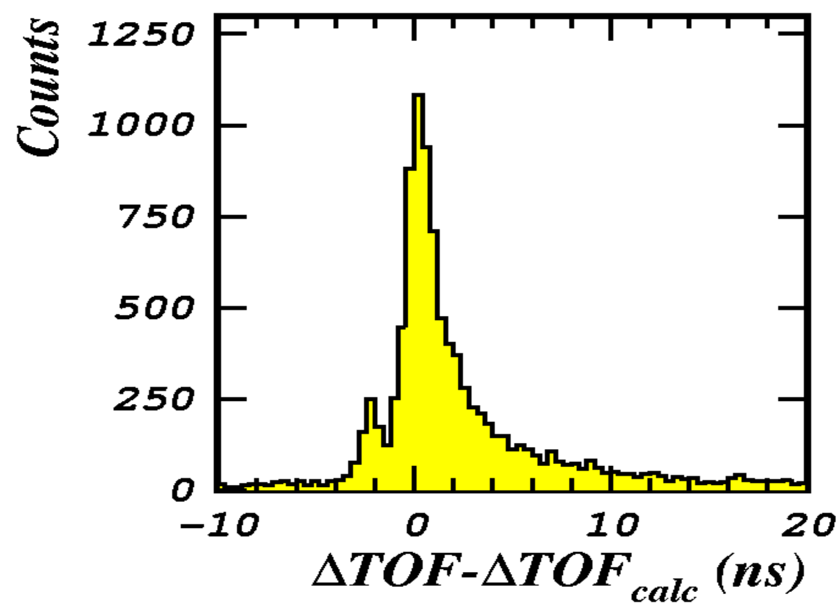

Cross-Ratio Analysis

Expressing asymmetry in terms of cross-ratio

$$\xi = AP = \frac{r-1}{r+1}$$

$$r = \sqrt{\frac{Y_{RU}Y_{LD}}{Y_{RD}Y_{LU}}}$$

minimizes systematic errors in efficiency, acceptance, and current.

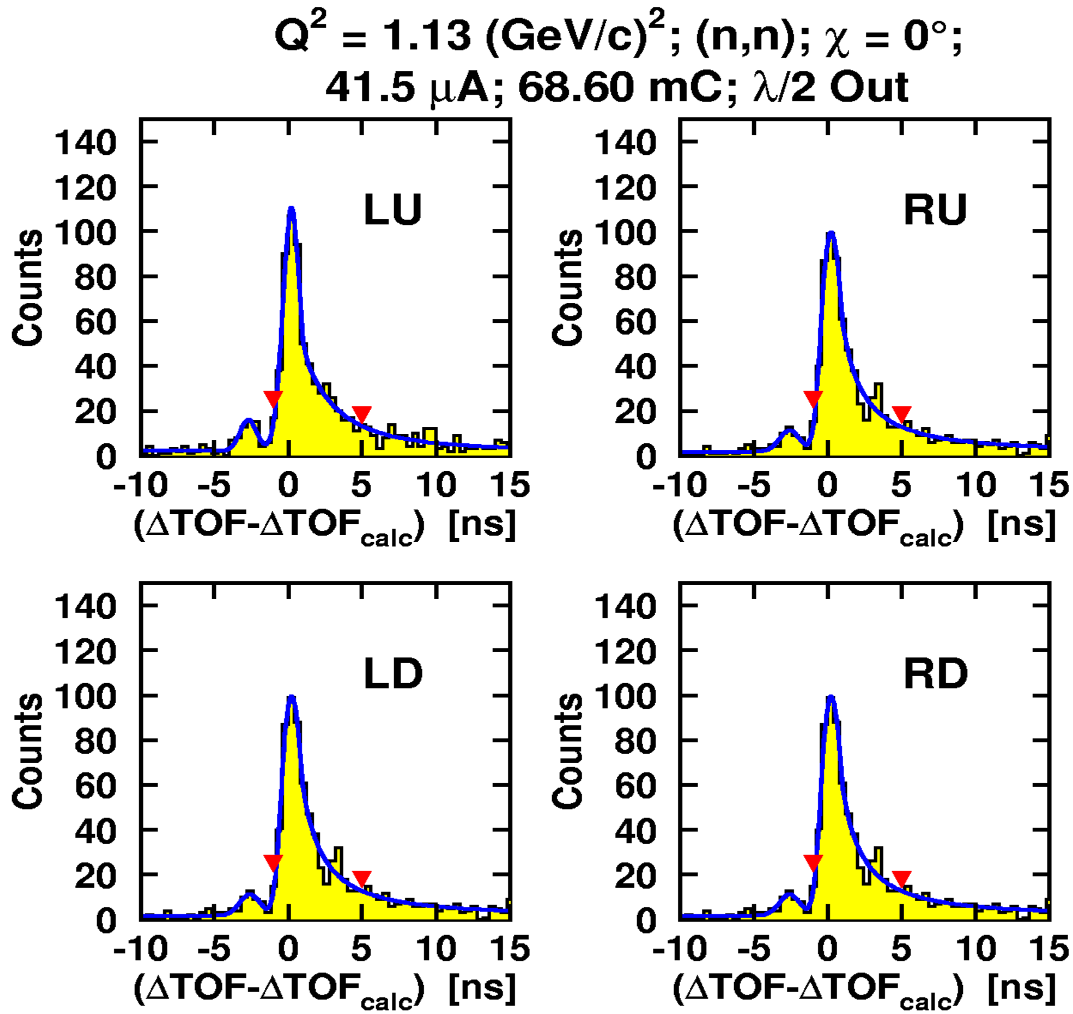

L/R: Beam Helicity
U/D: Up/Down Scattering

G_{En} from Precession Phase Shift

$$\xi \propto \sin(\chi + \delta) \Rightarrow g = \frac{G_E}{G_M} = -\tan\delta \sqrt{\frac{\tau(1+\varepsilon)}{2\varepsilon}}$$

- Up-down asymmetry ξ proportional to sideways polarization
- g depends on phase shift δ wrt precession angle χ
- Good consistency between *(n,n)* and *(n,p)* measurements

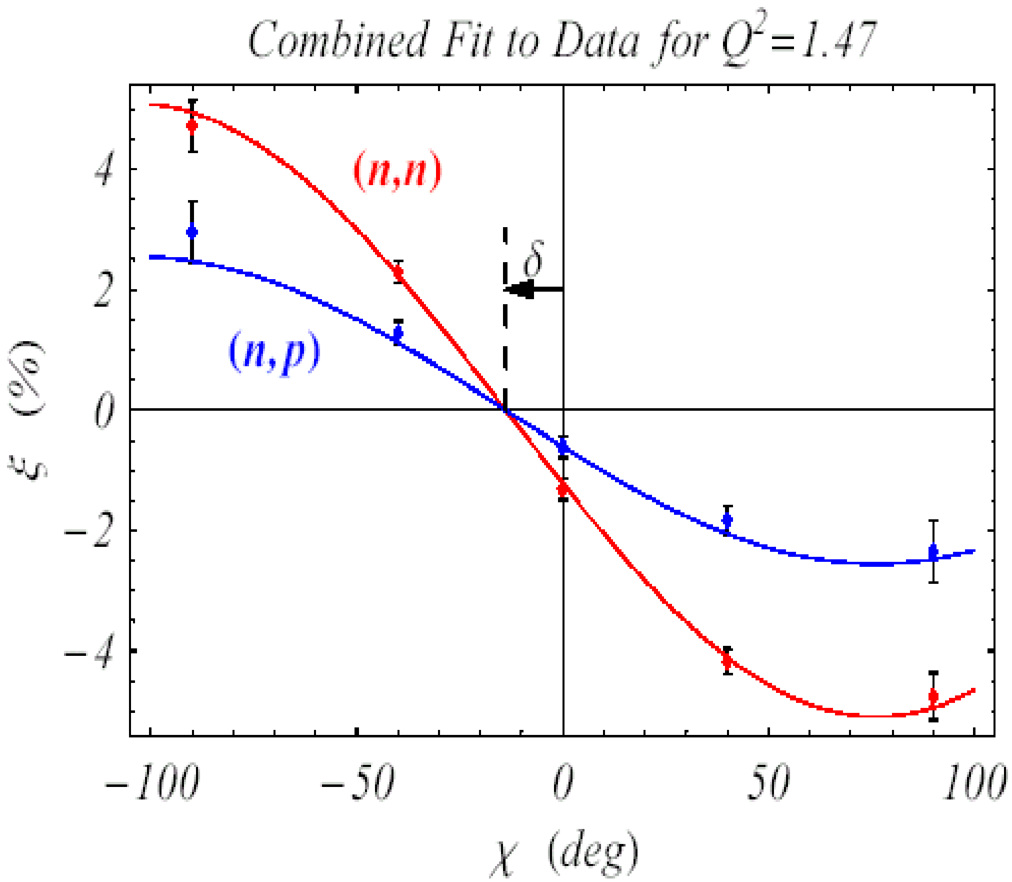

MAMI A1/2-99

- Recoil polarization in *d(e,e′n)*
- Designed for $Q^2 = 0.6$, 0.8
- Expect 10% statistical uncertainty

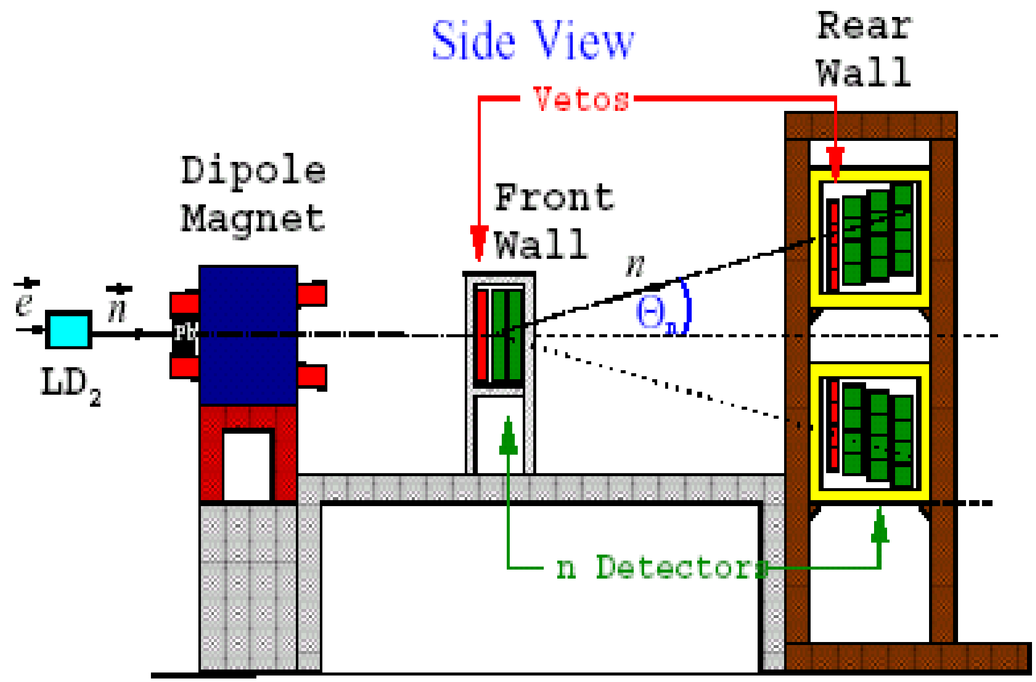

Target Polarization

$$\frac{G_E}{G_M} \propto \frac{A_S}{A_L}$$

target	Q^2	Lab
D	0.2	NIKHEF
$^{15}ND_3$	0.5, 1.0	JLab
^{3}He	0.4, 0.67	MAMI

- Dependence of quasifree cross section on target polarization analogous to recoil, but
  - rather different systematic errors
  - somewhat different model dependence
  - ^{3}He may give better figure of merit at large Q^2

Galster fit to polarization data

- New fit remarkably close to original Galster
- Paris fit well below data from polarization
- Mainz fit highest (omits lower ^{3}He point and JLab data)

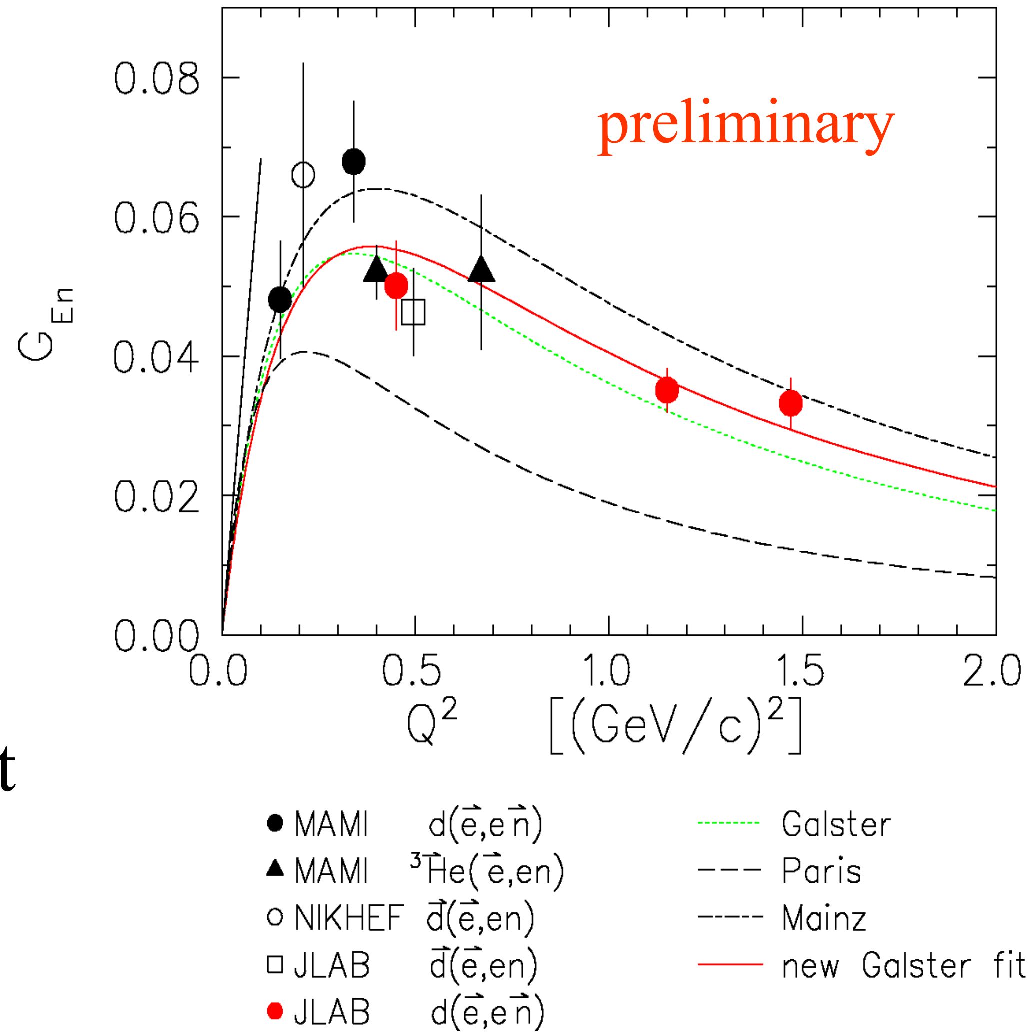

Representative Models

- VMD+pQCD
  - E. L. Lomon, nucl-th/0203081, version GKex(02S)
  - coupling to ρ, ω, φ, ρ′, ω′ with form factors
  - smooth extrapolation toward pQCD behavior
  - up to 14 parameters
- chiral soliton
  - G. Holzwarth, hep-ph/0201138, version B2
  - explicit ρ, ω. Adjustable "boost mass".
  - 5 parameters
- light-cone diquark
  - Ma *et al*., PRC 65 (02) 035205, set 3
  - scalar or vector diquark spectator
  - 5 parameters

- Point-form spectator approximation (PFSA)
  - R.F. Wagenbrunn et al., PL B511 (01) 33
  - parameters of GBE interaction determined by spectroscopy
  - pointlike CQ
  - no adjustable parameters for form factors
- light-front form of CQ model
  - S. Simula, nucl-th/0105024
  - OGE interaction
  - CQ form factors fitted to $Q^2 < 1$

Note: magnetic form factors normalized at $Q^2 = 0$.

Models vs. Electromagnetic Ratio

- Chiral soliton predicted linear g_p, but needs large boost mass for high Q^2 and does not fit g_n.
- VMD+pQCD fits well
- G_{En} particularly sensitive to scalar/vector diquark mixture or to small components of CQ wave function
- Deviations for CQ grow with Q^2, especially for neutron, probably due to multiquark currents.
- High Q^2 data for g_n important!

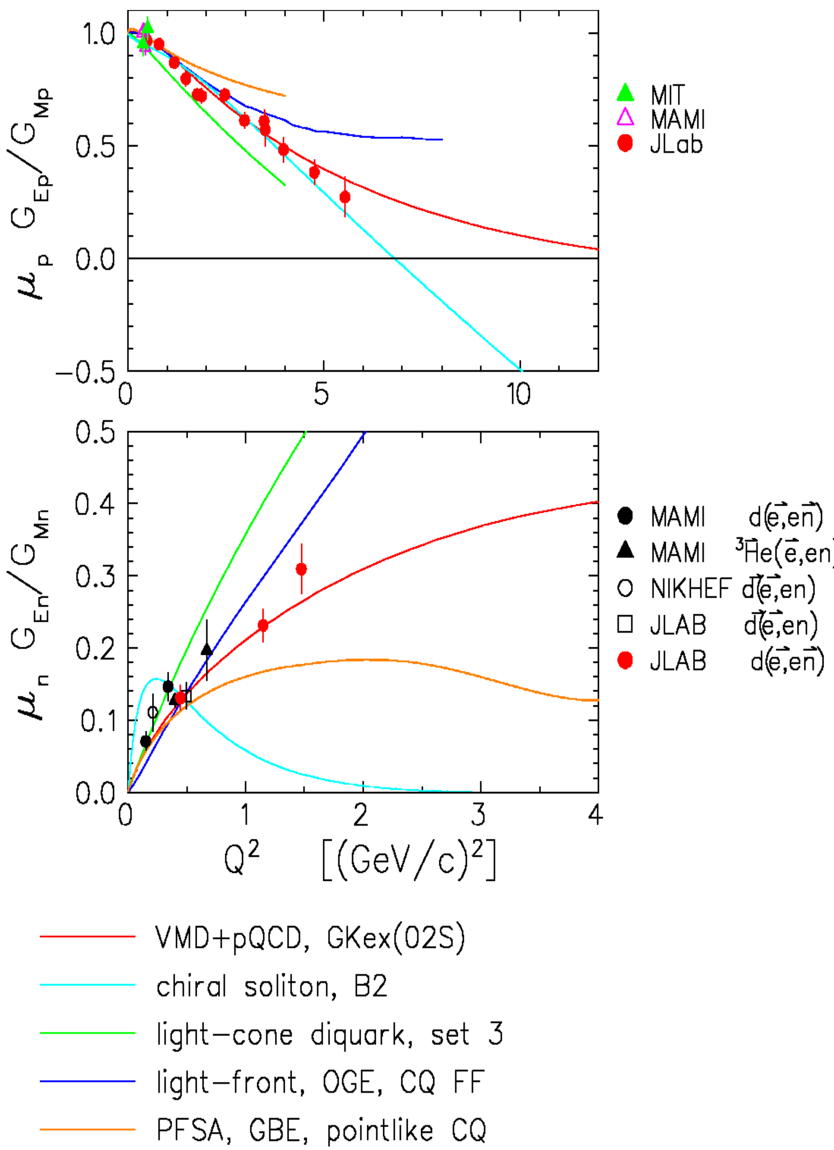

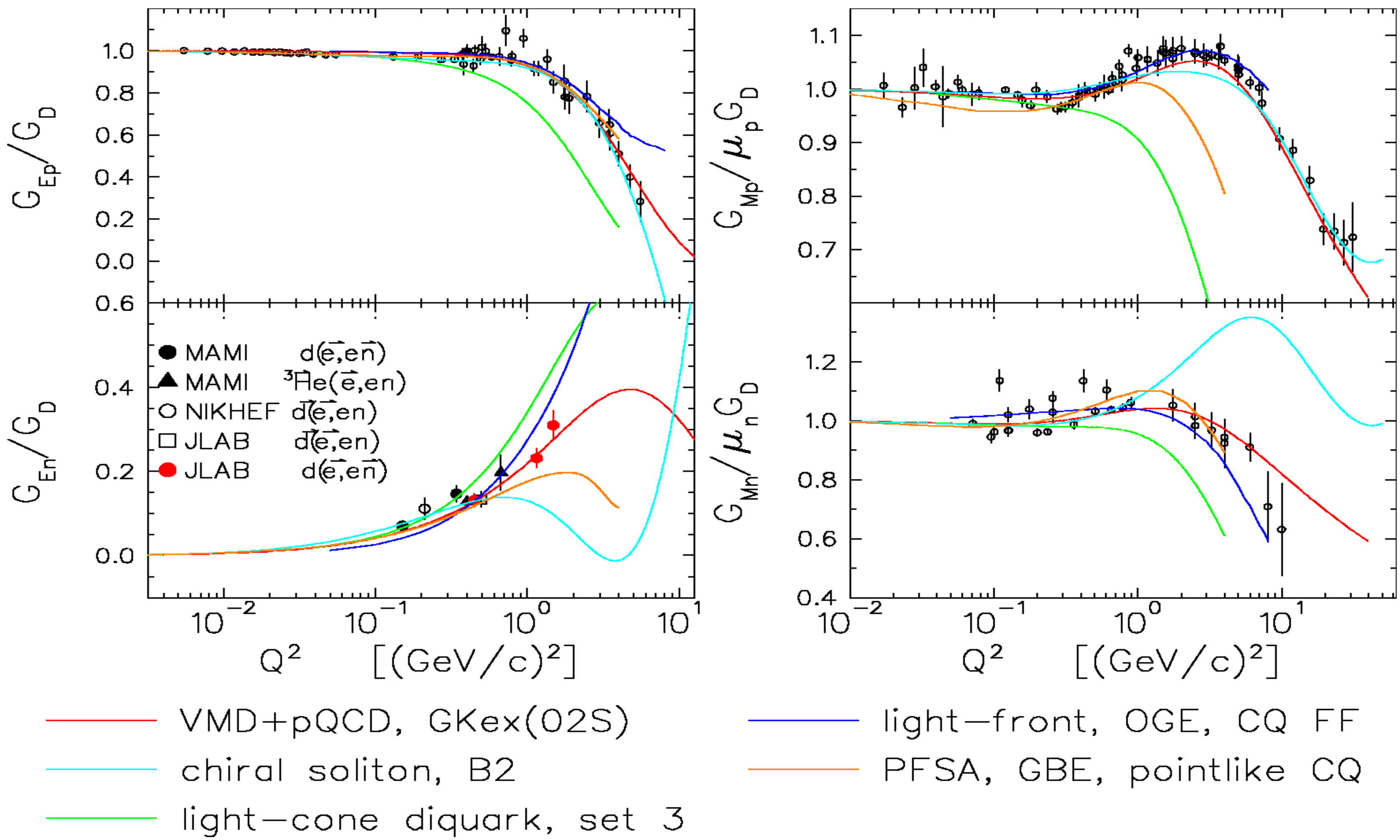

- Removing basic dipole reveals problems at large Q^2; diquark and soliton models seriously deficient.
- Relativistic CQ probably still needs form factors and/or multiquark currents at large Q^2.

Intrinsic Form Factor

If $\rho(r)$ is a rest-frame density, we would define an *intrinsic form factor* as

$$\tilde{\rho}(k) = \int_0^\infty dr\, r^2 j_0(kr)\rho(r)$$

Then, if we knew how to obtain $\rho(k)$ from $G(Q^2)$ we could obtain $\rho(r)$ using

$$\rho(r) = \tfrac{2}{\pi}\int_0^\infty dk\, k^2 j_0(kr)\tilde{\rho}(k)$$

Unfortunately, elastic scattering connects different states and boosts depend upon interactions. Therefore, the relationship between *transition* form factor and *static* density is *model dependent*.

Nonrelativistic inversion

Naively one interprets Sachs form factors as Fourier transforms of charge and magnetization densities

$$\rho_{ch}^{NR}(r) = \tfrac{2}{\pi}\int dQ\ Q^2 j_0(Qr) G_E(Q^2)$$

$$\mu\rho_{m}^{NR}(r) = \tfrac{2}{\pi}\int dQ\ Q^2 j_0(Qr) G_M(Q^2)$$

and obtains radii from the low Q^2 expansion

$$G(Q^2) = G(0)\left(1 - \frac{Q^2\left\langle r^2\right\rangle}{6} + \cdots\right)$$

but every Q^2 represents a different Breit frame.

Relativistic Inversion

Several models suggest

$$\tilde{\rho}_{ch}(k) = G_E(Q^2)(1+\tau)^{\lambda_E}$$

$$\tilde{\rho}_m(k) = G_M(Q^2)(1+\tau)^{\lambda_M}$$

Author	**Model**	$\boldsymbol{\lambda_E}$	$\boldsymbol{\lambda_M}$
Licht&Pagnamenta	cluster	1	1
Mitra&Kumari	cluster	2	2
Ji, Holzwarth	soliton	0	1

where

$$k^2 = \frac{Q^2}{1+\tau} \qquad \tau = \left(\frac{Q}{2m}\right)^2$$

describes Lorentz contraction of local Breit frame. Momentum transfer Q samples much smaller frequency k. Maximum k

$$0 \le Q^2 \le \infty \Rightarrow k \le 2m$$

limited by Compton wavelength -- *zitterbewegung* limits resolution

High Q^2 Behavior

The asymptotic expansion takes the form

$$G(Q^2) \rightarrow \left(\frac{k_m}{Q}\right)^{2\lambda} \left(\tilde{\rho}(k_m) + a_1 \left(\frac{k_m}{Q}\right)^2 + a_2 \left(\frac{k_m}{Q}\right)^4 + \cdots \right)$$

where $k_m = 2m$ and a_n involve derivatives of order n and lower. Consistency with pQCD requires λ=0,1,2 plus constraints on on the intrinsic f.f. at the limiting frequency:

- λ=0: f.f. and derivative vanish at k_m
- λ=1: node at k_m
- λ=2: nonzero at k_m

Therefore, Mitra/Kumari model (λ=2) offers most natural extrapolation to pQCD.

Dipole and Galster Models

- Relativistic inversion impossible with λ=0
- λ=1 density singular at origin and converges slowly
- NR and λ=2 give cusp at origin
- Models similar for r>0.2 fm (Compton wavelength)

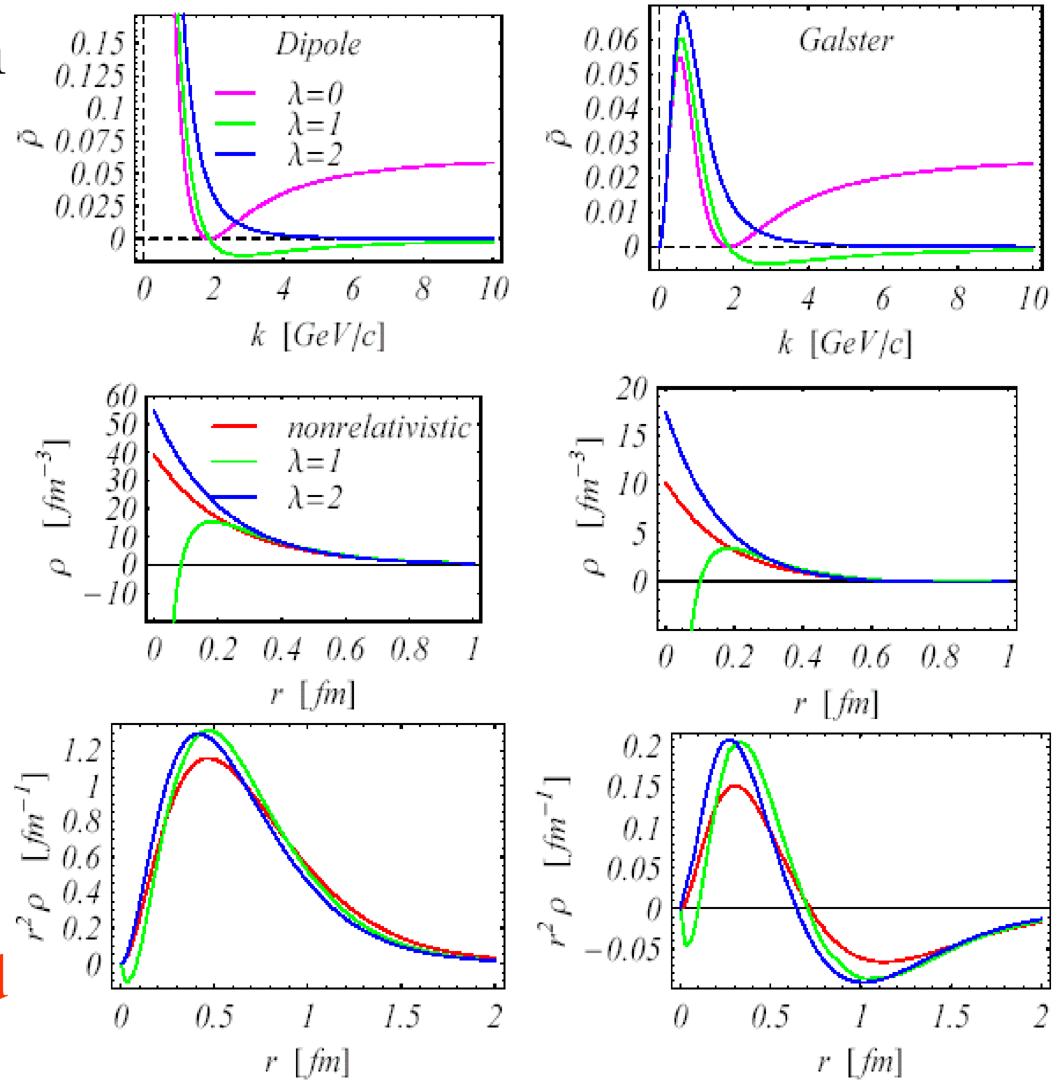

Asymptotic decline should be faster than k^{-4}.

Form Factor for Gaussian Density

$$\tilde{\rho}(k) = Exp\left(-\left(kb/2\right)^2\right)$$

$$G(Q^2) = \frac{\tilde{\rho}(k)}{(1+\tau)^2}$$

$$k^2 = \frac{Q^2}{1+\tau} \qquad \tau = \frac{Q^2}{4m^2}$$

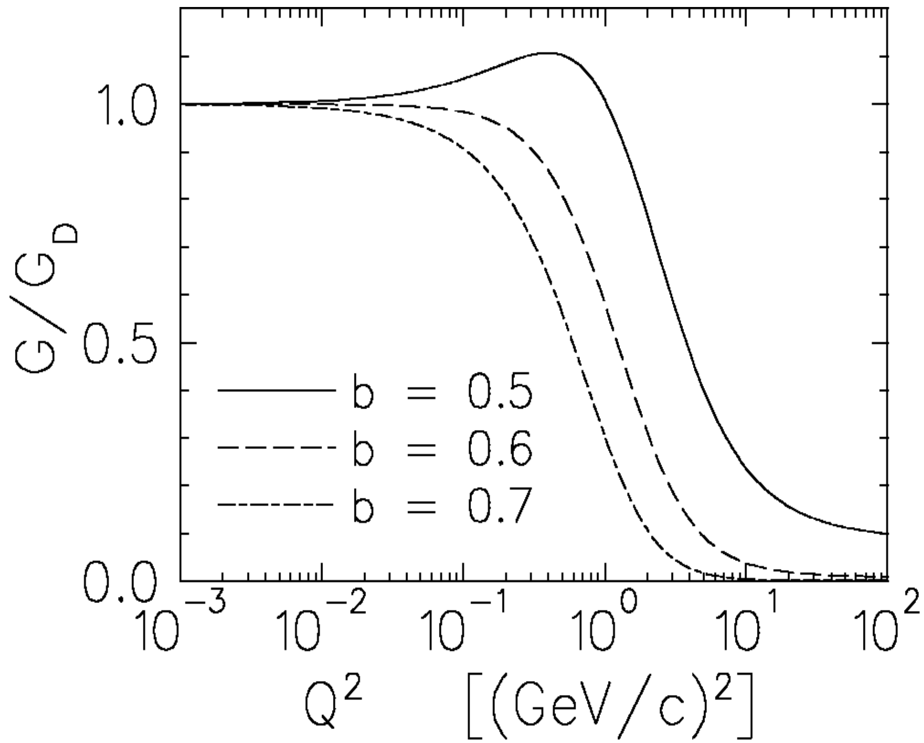

- Constituent quark models suggest Gaussian intrinsic density.
- Consistent with dipole for low Q^2, pQCD for high Q^2
- Transition region for $Q^2 \sim$ few (GeV/c)^2 similar to G_{Ep}, G_{Mp}
- Can improve fit with small modifications of Gaussian density.

Linear Expansion Analysis

Minimize model dependence by expansion in complete basis:

$$\rho(r) = \sum_n a_n f_n(r) \qquad \tilde{\rho}(k) = \sum_n a_n \tilde{f}_n(k)$$

Basis functions for

- Fourier-Bessel expansion (FBE) localized in k
- Laguerre-Gaussian expansion (LGE) better at large r

Fit coefficients to:

- data → statistical uncertainties
- large k pseudodata → incompleteness error
- large r pseudodata → stabilizes moments

Incompleteness error

- Inversion of Fourier transform requires infinite k but spacelike Q^2 limited to $k<2m$.
- Experimental data limited to $Q<Q_{max}$, corresponding to $k<k_{max}<2m$.
- Assume asymptotic form factor below k^{-4} envelope

$$\delta\widetilde{\rho}(k) = \sqrt{\tfrac{1}{3}}\,\widetilde{\rho}_{\text{lim}}(k) \qquad \widetilde{\rho}_{\text{lim}}(k) = \left|\widetilde{\rho}(k_{\text{max}})\right|\left(\frac{k_{\text{max}}}{k}\right)^4$$

• Pseudodata, uniformly distributed within envelope, permits many expansion coefficients to be fitted.

• Incompleteness error estimates flexibility in density permitted by ignorance of form factor at very large k.

• Minimum uncertainty limited by *zitterbewegung*.

Data Selection

- Emphasize polarization data wherever available
  - rely on JLab recoil polarization, omit SLAC data, for G_{Ep} at large Q^2.
- For G_{En} use recoil and target polarization data:
  - at low Q^2 correct for FSI, structure, etc.
  - also use Schiavilla&Sick analysis of quadrupole form factor
- Use coincidence data for G_{Mn} at low Q^2.

LGE fits to Sachs Form Factors

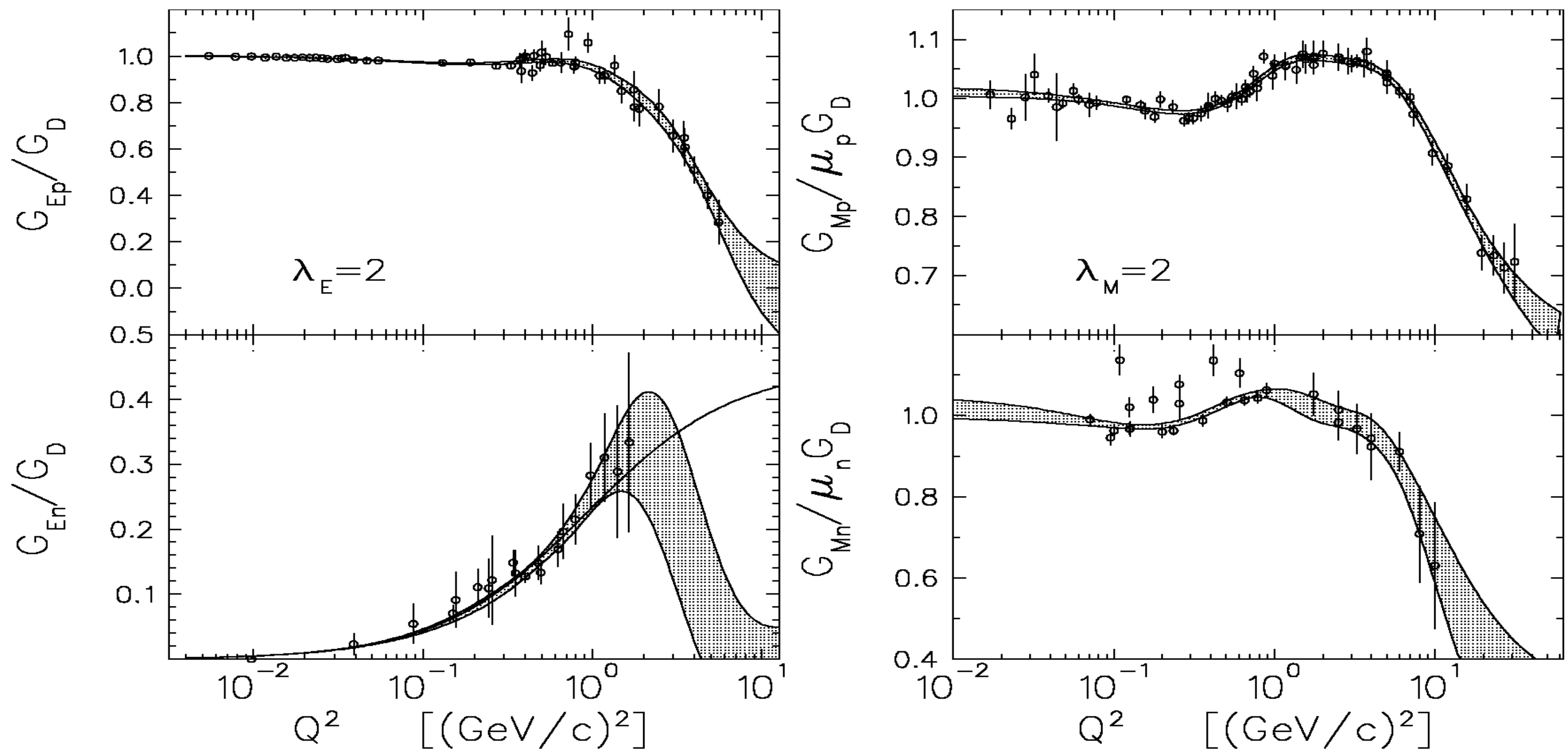

- Good fits, same for FBE as LGE, insensitive to details
- Bands show statistical quality in data range, incompleteness at larger Q^2. Uncertainty in extrapolation depends upon λ.
- G_{En} data consistent with Galster, but model prefers lower extrapolation.

Intrinsic Form Factors

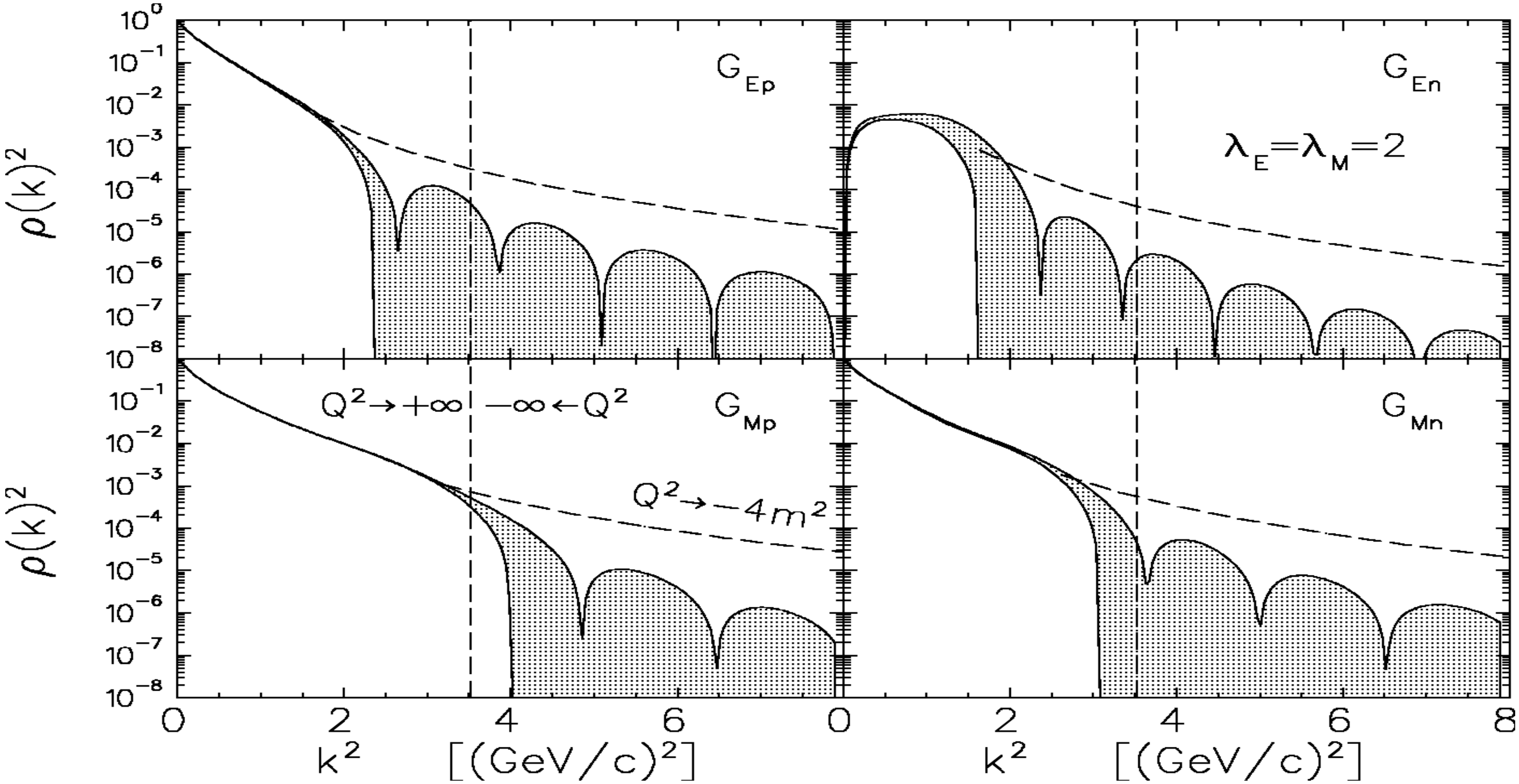

- Electron scattering with $0<Q^2<\infty$ limited to $k<2m$.
- Ignorance in unmeasured and inaccessible regions contribute to incompleteness error.
- k^{-4} bound removes cusp, stabilizes density.

Nucleon electromagnetic ratio

- Proton ratio approximately linear for $1 \leq Q^2 \leq 6$, but LGE suggests later sign change
- Insufficient data for neutron at large Q^2.

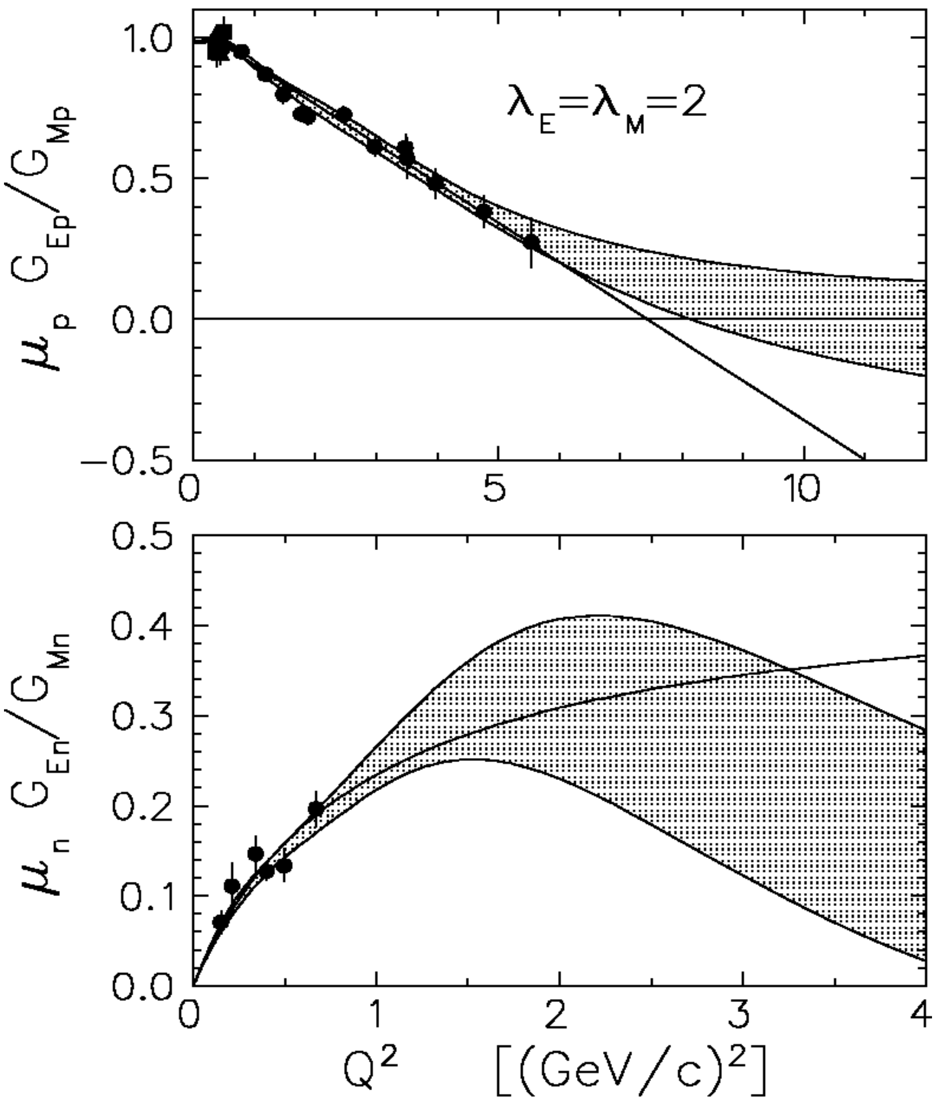

Approach to pQCD scaling

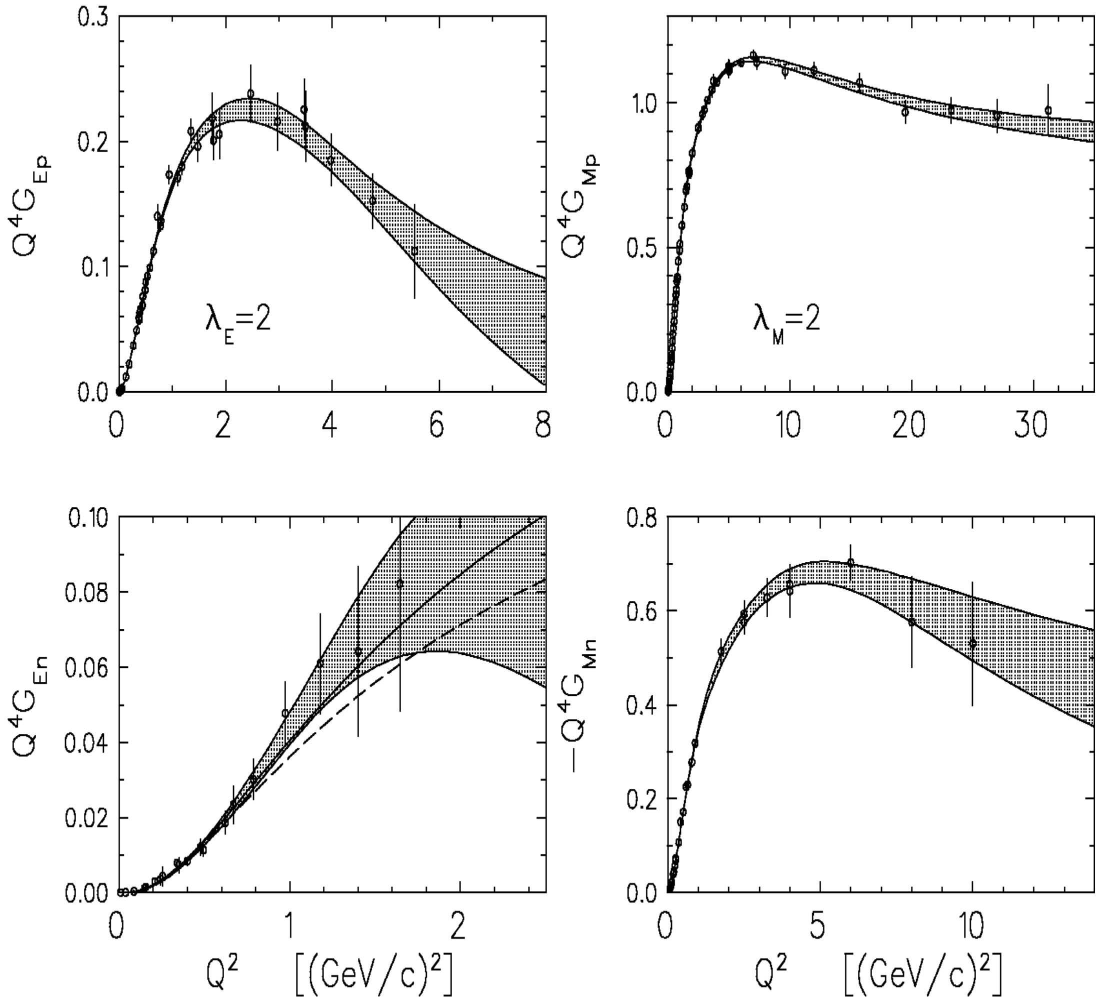

- G_{Mp} appears to scale for $Q^2 > 20$ (GeV/c)^2
- G_{Ep} is still far from scaling regime, may change sign
- G_{Mn} approaching scaling regime
- Need larger Q^2 for G_{En}, but shouldn't expect scaling until about 20 (GeV/c)^2

Helicity Conservation

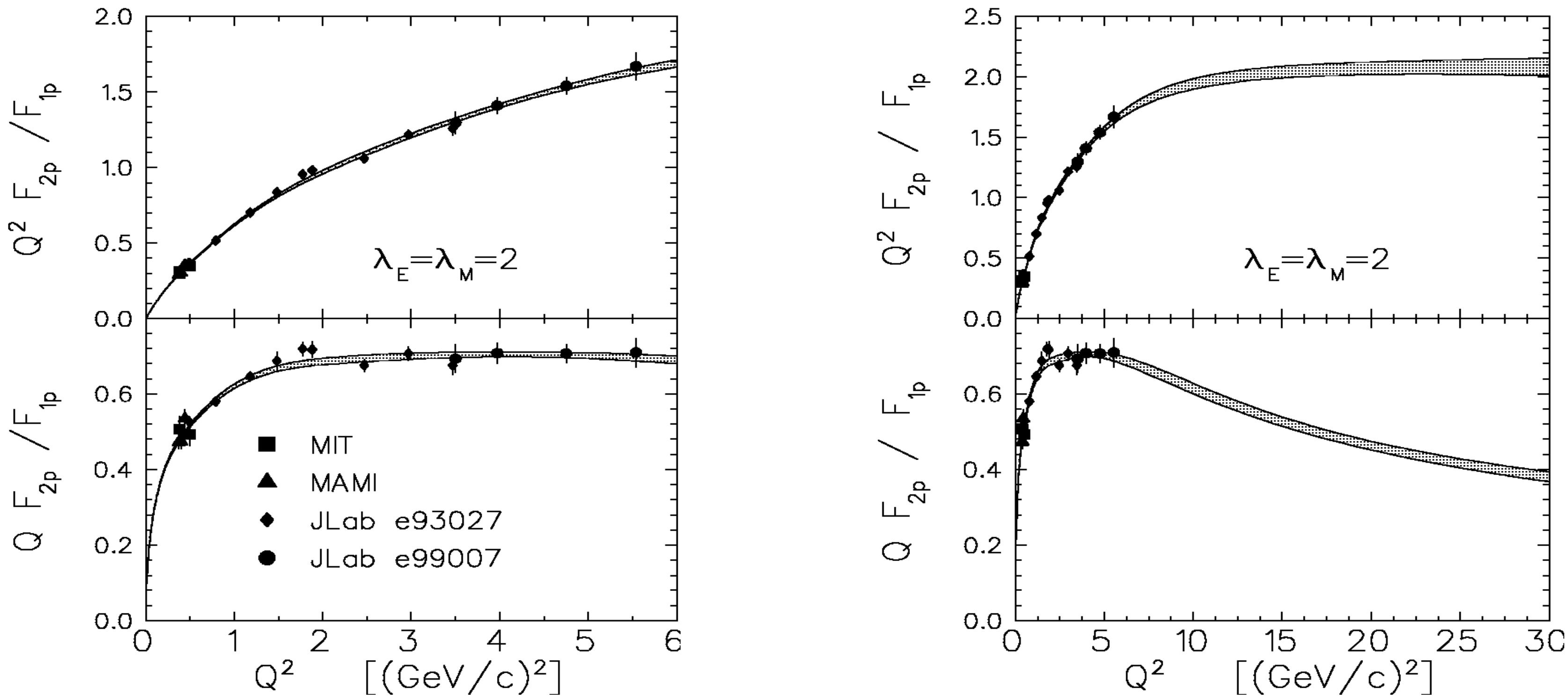

- Jlab data appear to show F_{2p}/F_{1p} scaling Q^{-1} with instead of Q^{-2}
  - Violation of helicity conservation for intermediate Q due to orbital angular momentum (Ralston, Miller, ...)
- Fit with λ=2 permits extrapolation

Larger Q^2 range remains compatible with helicity conservation

Densities using $\lambda_E = \lambda_M = 2$

- Proton charge broader than magnetization
- Magnetization slightly broader for n than p
- Incomplete cancellation for n charge leaves positive core and negative surface
- Need larger Q^2 to reduce uncertainty in neutron charge density -- interior dominated by incompleteness.

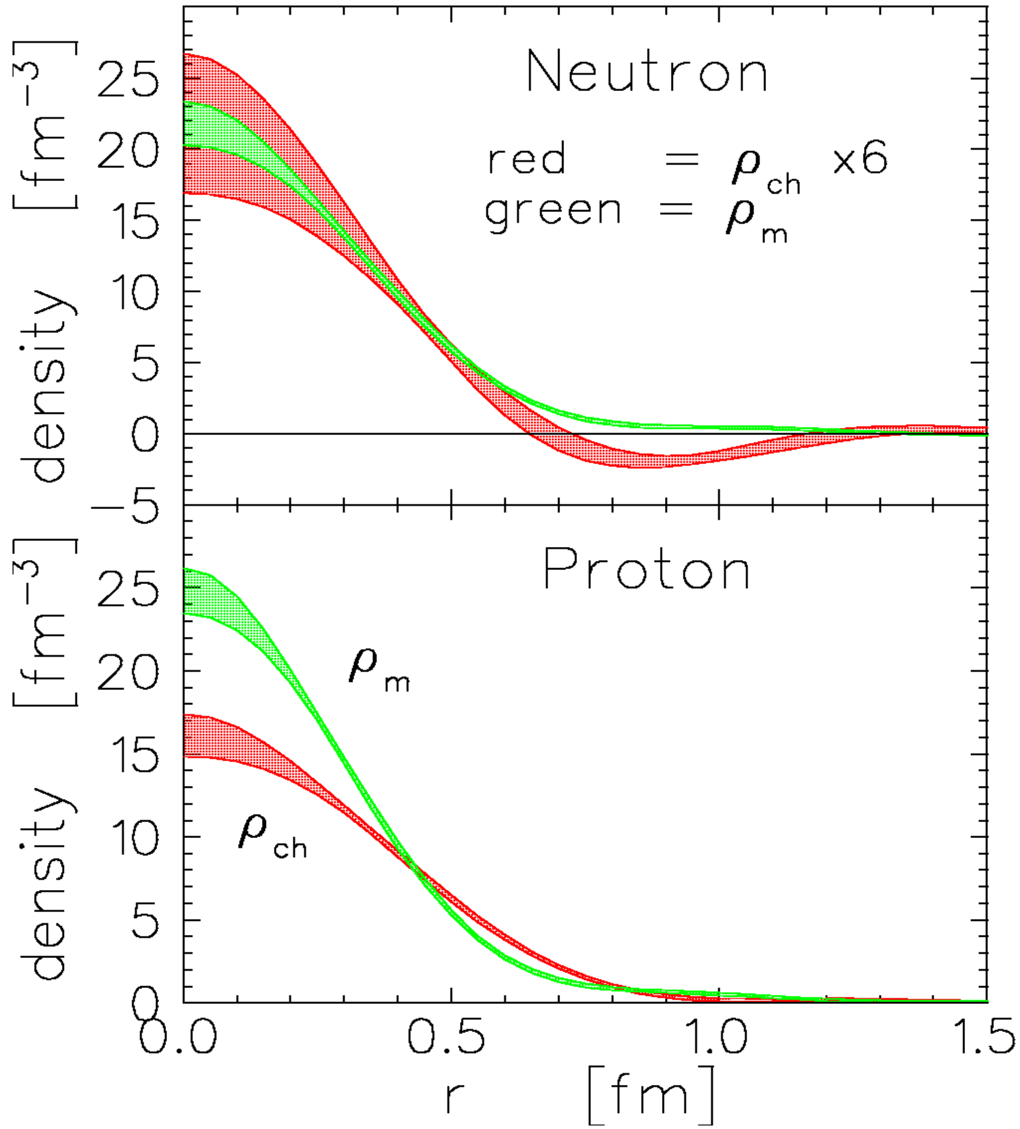

Magnetization Densities

- Very similar, but slightly broader for n than p.
- Problems in neutron data may affect oscillation at largest radius, but intermediate oscillation is stable.
- Feature near 1 fm may be due to D-state admixture from quark hyperfine interaction.

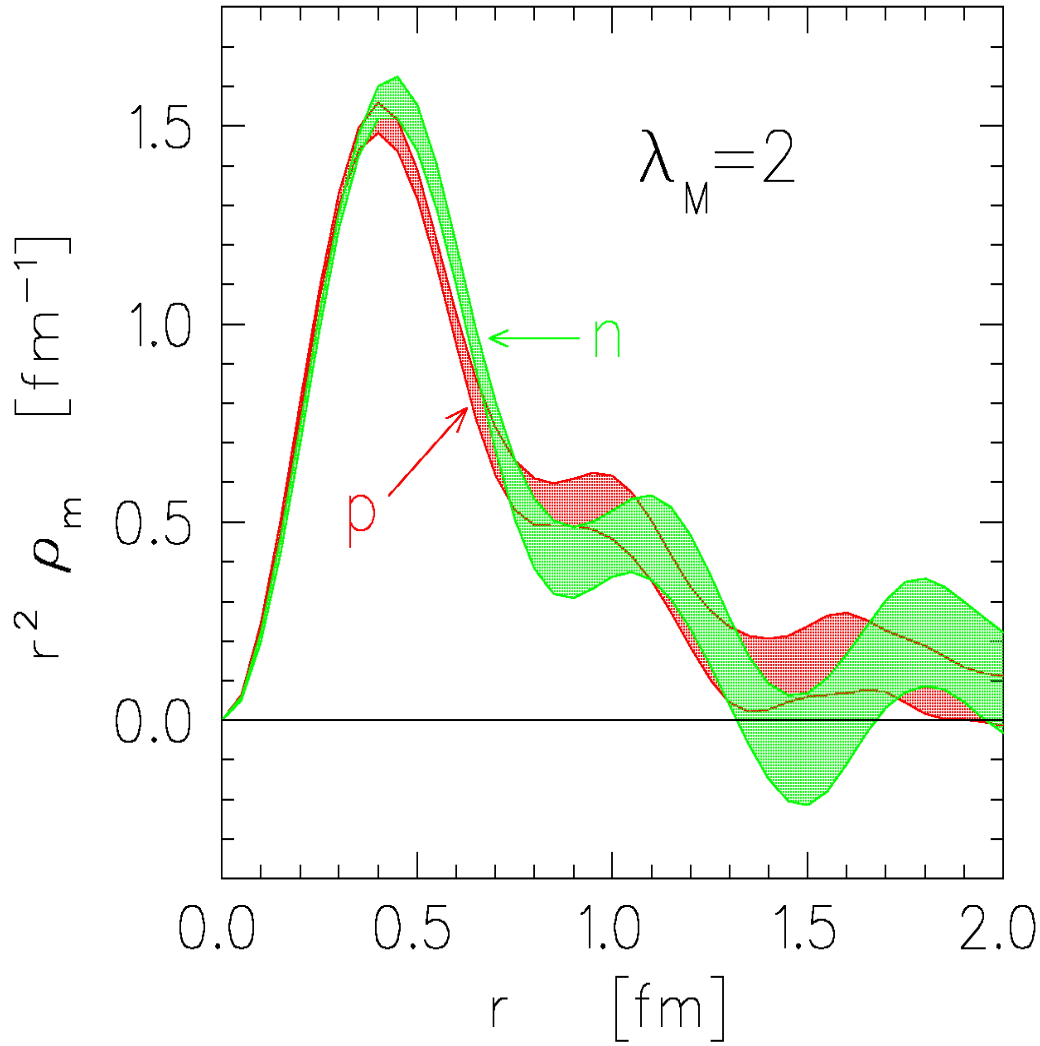

Stability of Fitted Densities

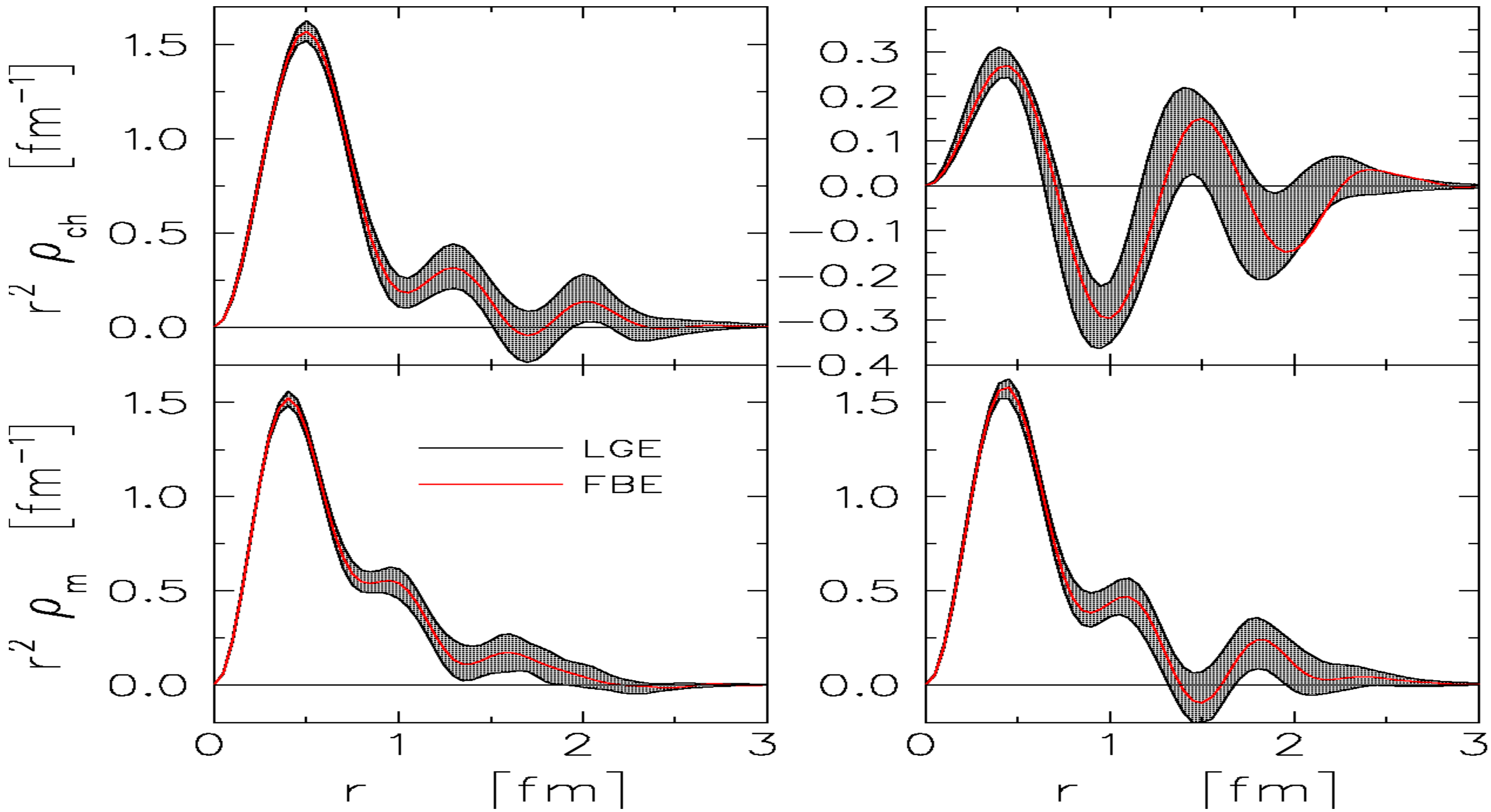

- Densities independent of basis (LGE vs. FBE) and details of fitting procedure.
- Small oscillations are stable features of data.

Impact of JLab Proton Data

- Model encourages decrease in G_{Ep}/G_D to remove cusp in density at origin
  - Need larger Q^2 to look for sign change
- JLab f.f. and density softer than SLAC results
  - Oscillation in $r^2\rho$ stable (same in FBE, LGE, etc.)
  - New "super Rosenbluth" experiment to check

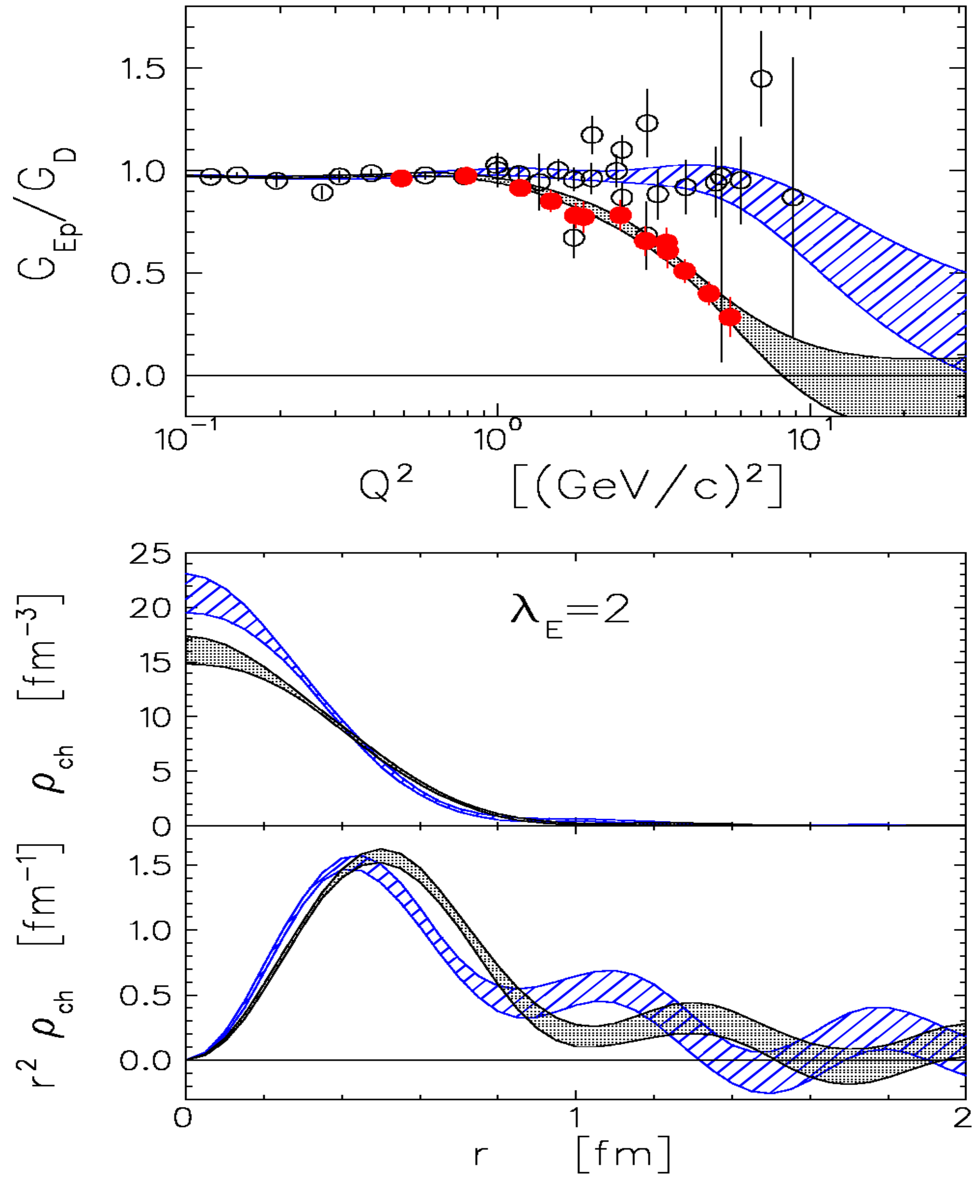

Impact of e93-038

- New data improves error band
- Interior band dominated by incompleteness
- New Galster fit above original

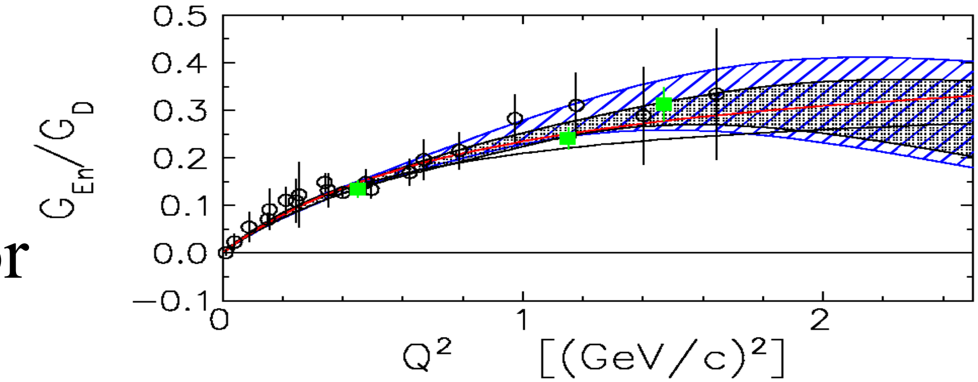

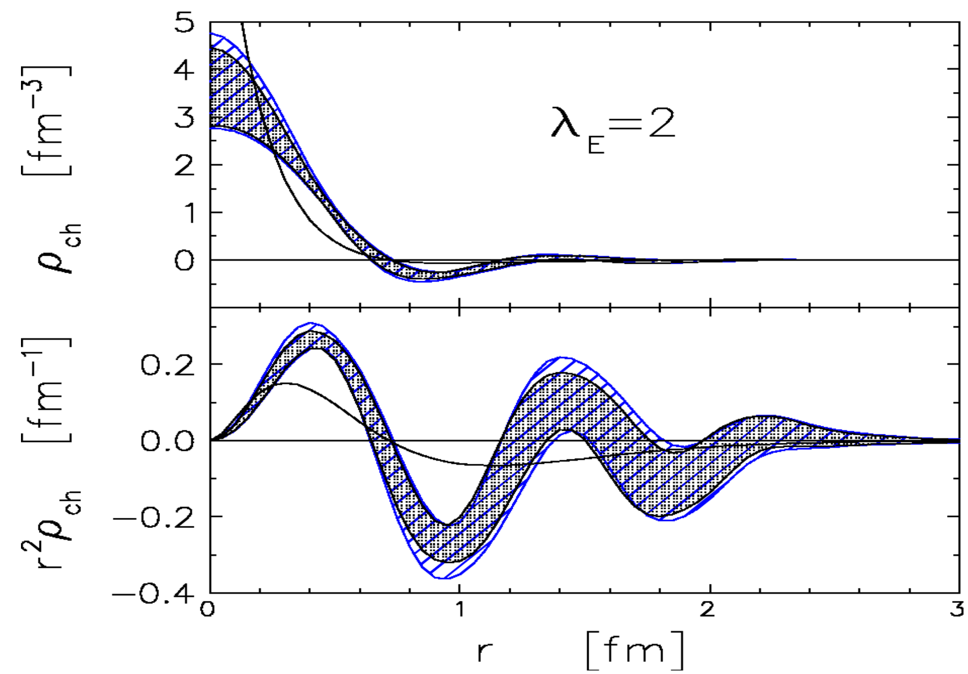

Relativistic vs. Nonrelativistic neutron density

- Use λ=0 to simulate nonrelativistic inversion
- Nonrelativistic inversion produces cusp at origin
- Relativistic inversion yields softer density w/o cusp

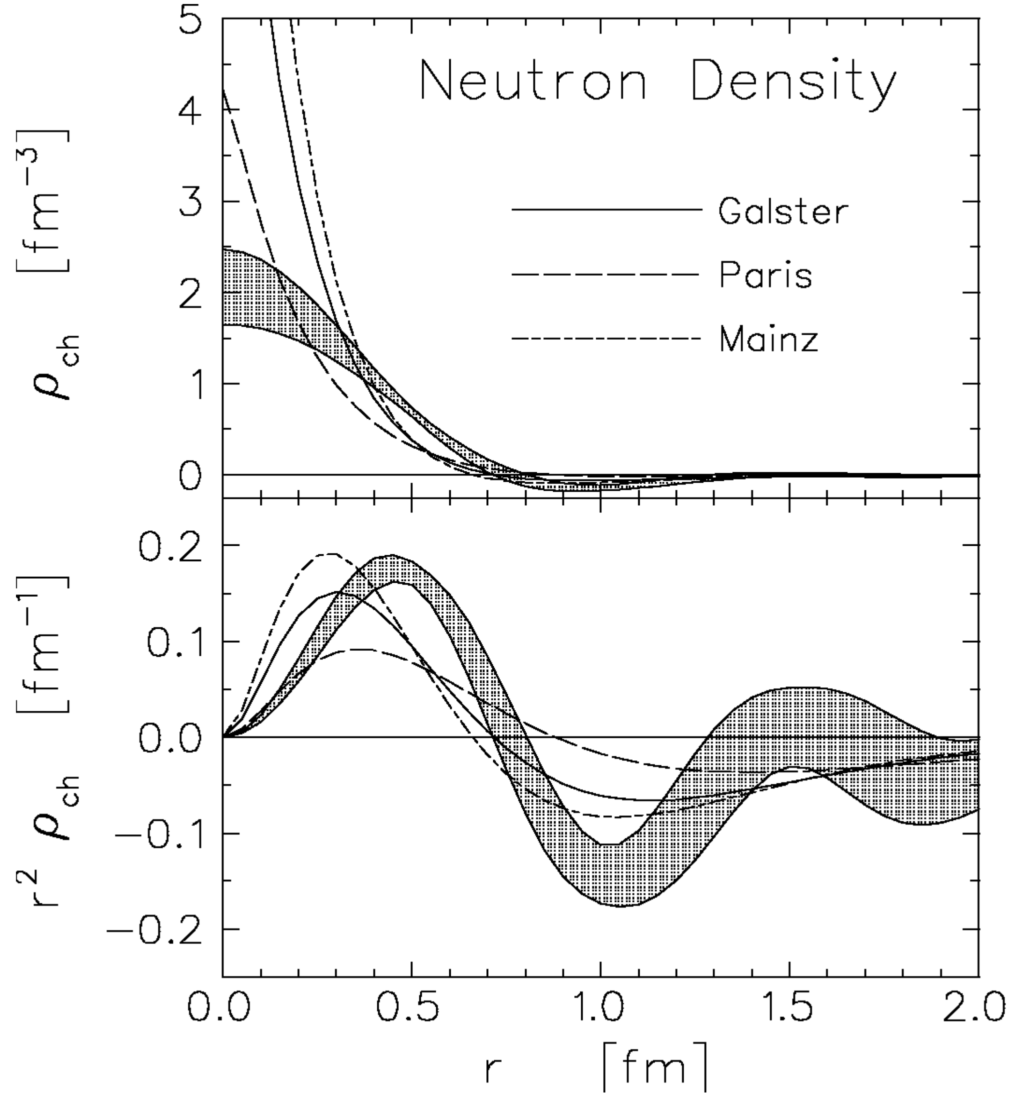

Simple Model for Quark Densities

Using isospin symmetry and 2 flavors, the charge densities become

$$\rho_p(r) = \tfrac{4}{3}u(r) - \tfrac{1}{3}d(r)$$
$$\rho_n(r) = -\tfrac{2}{3}u(r) + \tfrac{2}{3}d(r)$$

$$\Rightarrow$$

$$u(r) = \rho_p(r) + \tfrac{1}{2}\rho_n(r)$$
$$d(r) = \rho_p(r) + 2\rho_n(r)$$

where u represents up (down) quarks and d represents down (up) quarks in the proton (neutron). Each quark distribution is normalized to unity. Quarks should give positive and antiquarks negative contributions.

Quark densities using λ=2

- Distribution of like quarks broader than unlike quark
- Negative d near 1 fm consistent with antiquark content of pion cloud

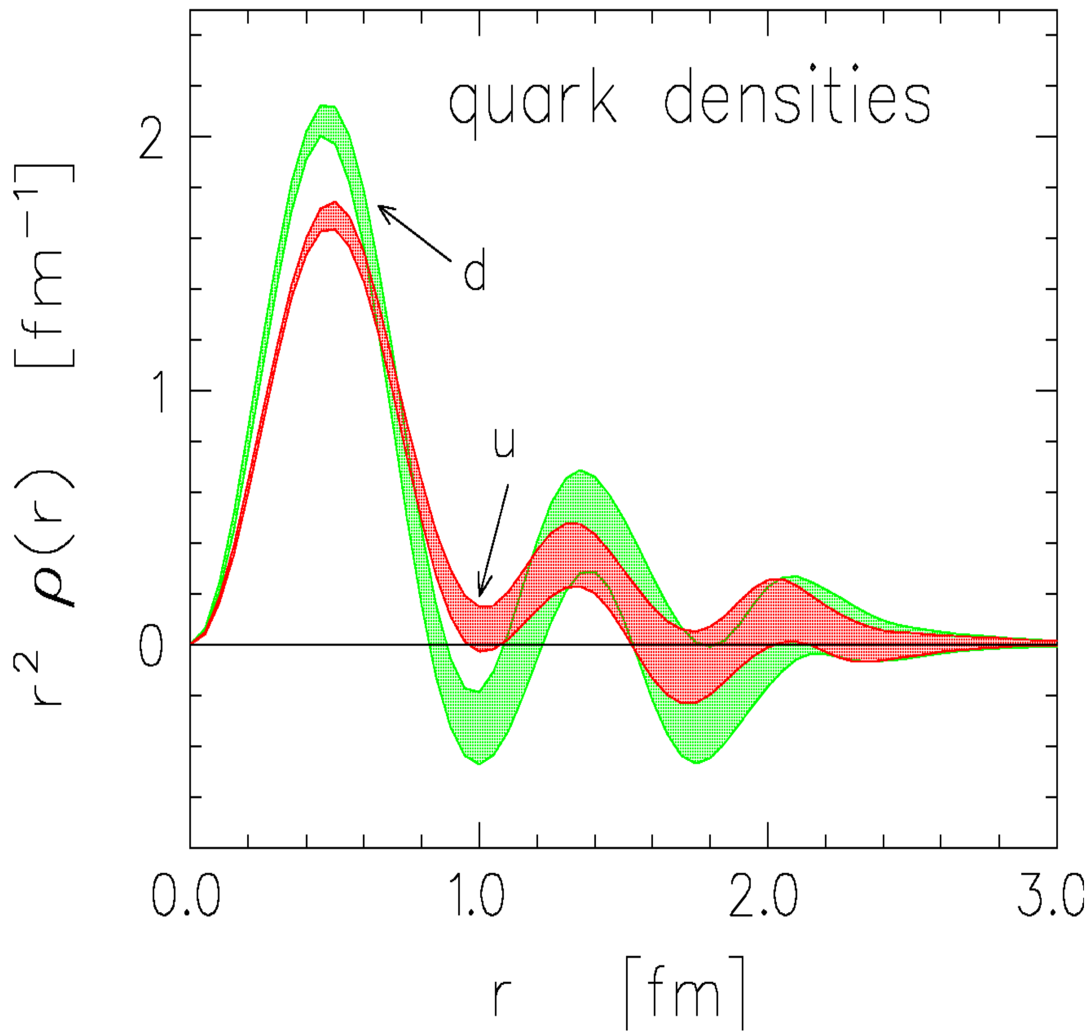

Discrete Ambiguities

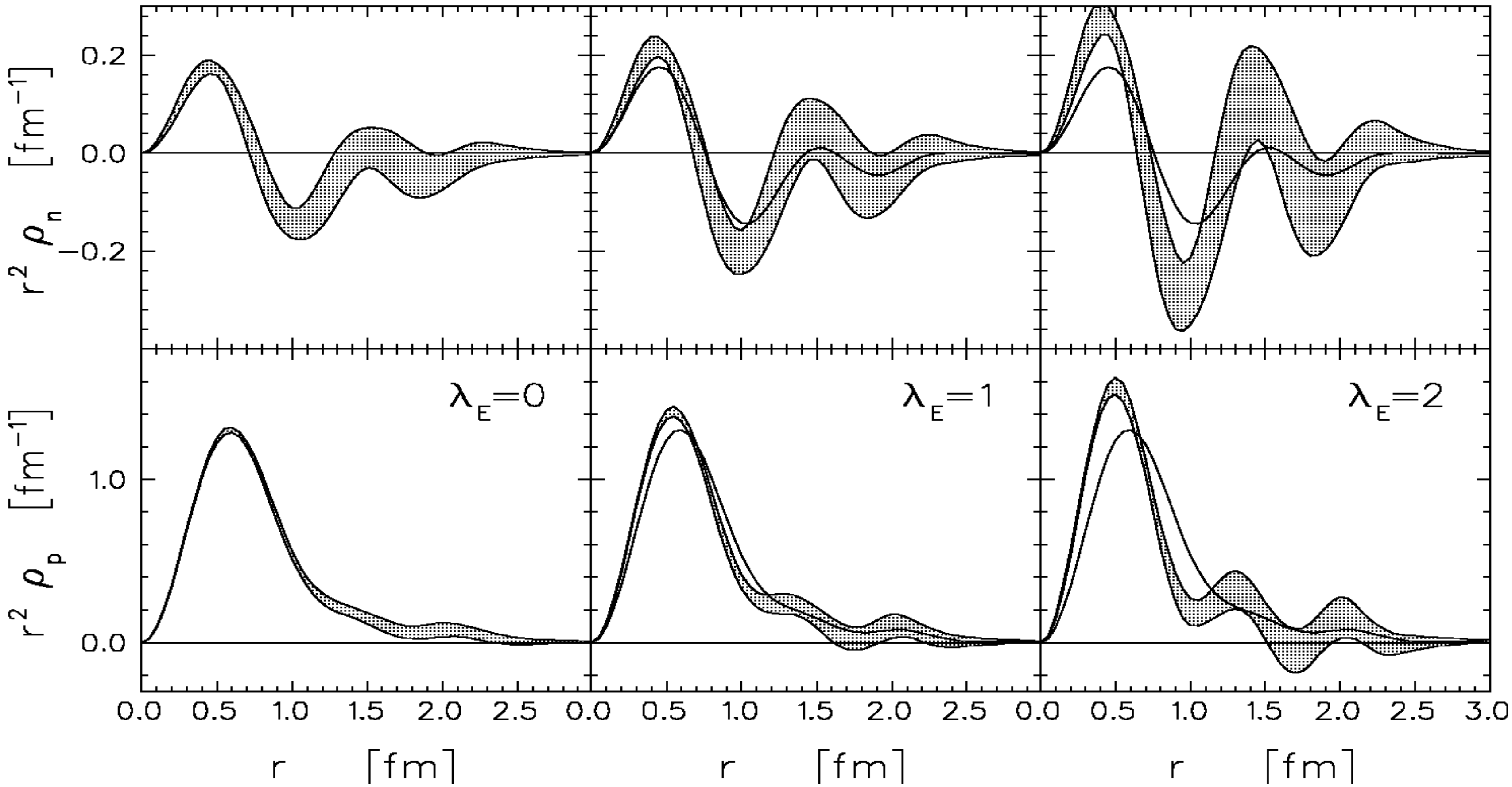

- Fit to Sachs data insensitive to λ, but decrease of λ equivalent to convolution with *zitterbewegung* f.f., resulting in smoother, broader density.

Quark densities using λ=0

- Both densities broadened wrt λ=2, but conclusion that distribution of like quarks broader than unlike quark is preserved.
- General features depend upon positive core, negative surface for neutron

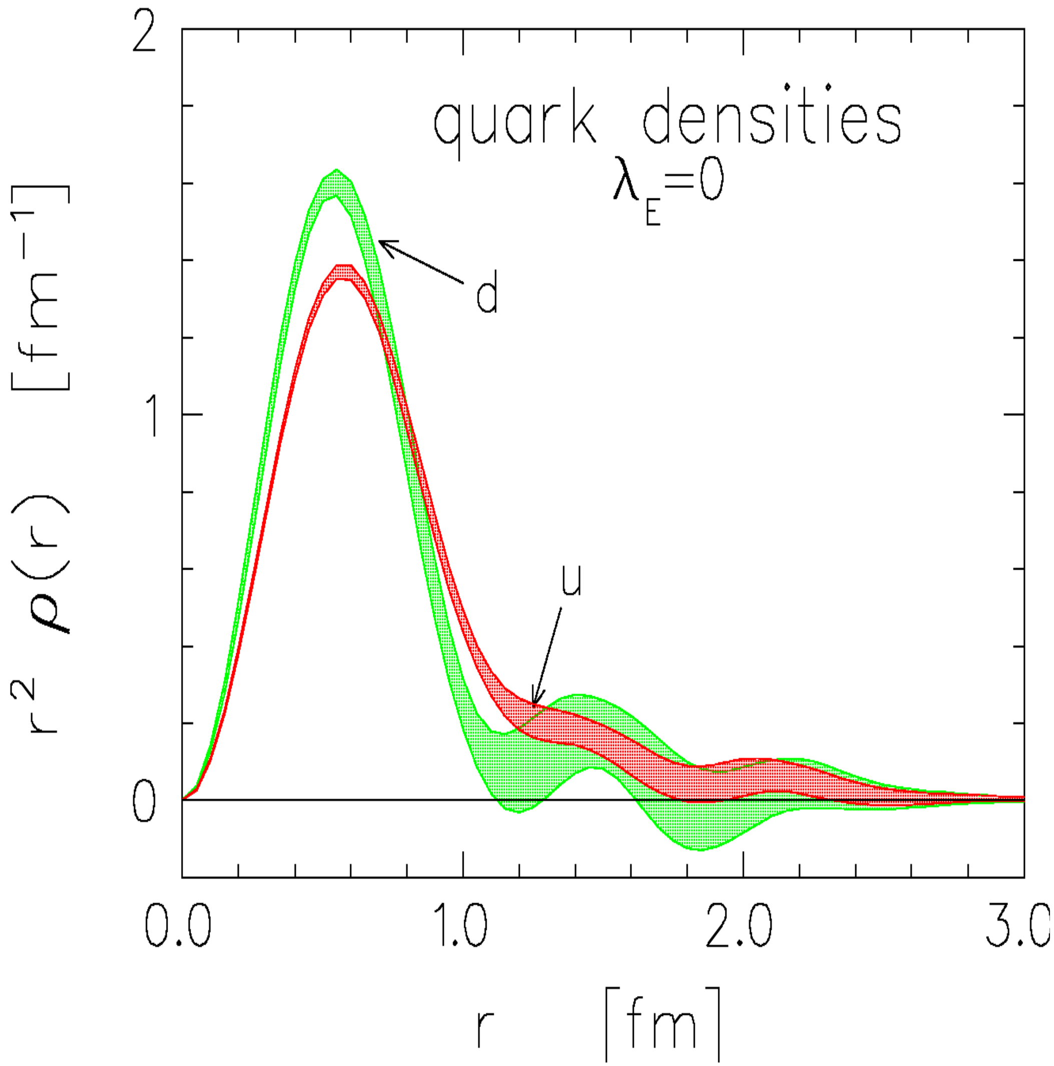

Low Q^2 Behavior

Moments of the intrinsic density are related to the low Q^2 properties of Sachs form factors by:

$$M_\alpha = \int dr\, r^{2+\alpha} \rho(r)$$

$$M_0 = G(0)$$

$$M_2 = -6 \frac{dG(Q^2)}{dQ^2}\bigg|_{Q^2 \to 0} - \frac{3\lambda}{2m^2} G(0)$$

$$R_\lambda^2 = M_2 / M_0 \qquad (M_0 \neq 0)$$

Model-dep. *transition radius* subject to a ***discrete ambiguity***, 0.066 λG(0) fm^2, that persists at $Q^2 \to 0$. Does not affect neutron charge radius squared, M_{2n}.

Sachs radius: $\xi^2 = -6 \frac{d \ln G(Q^2)}{dQ^2}\bigg|_{Q^2 \to 0} = \frac{M_2}{M_0} + \frac{3\lambda}{2m^2}$ is model indep.

Proton Charge Radius

method	M_0	R_λ (fm)	ξ (fm)
Simon	[1.0]	0.862(12)	
LGE 0	[1.0]	0.862(06)	
LGE 0	1.003(1)	0.879(11)	0.879(11)
LGE 1	1.003(2)	0.843(12)	0.881(12)
LGE 2	1.003(2)	0.804(13)	0.883(14)
Lamb			0.880(10)

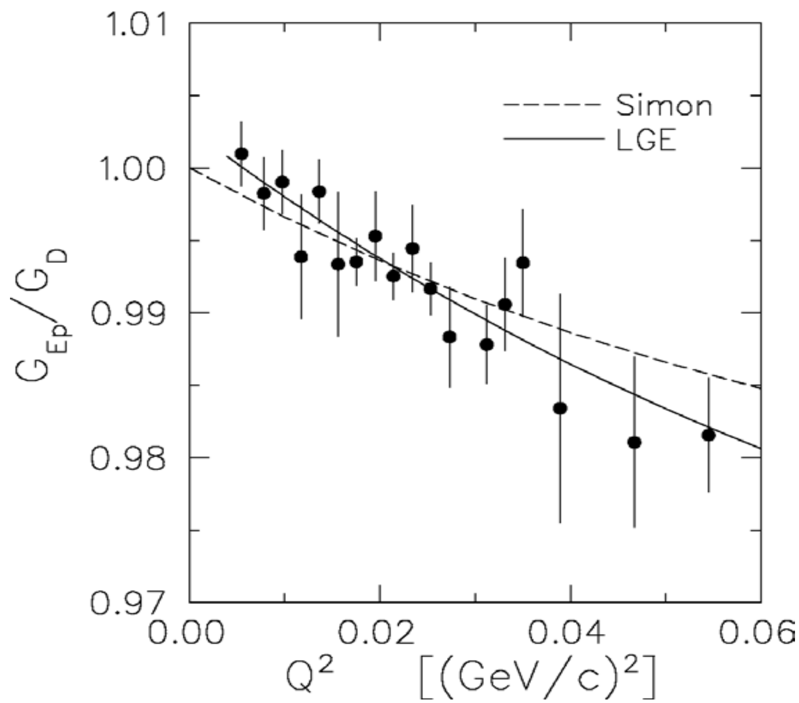

- Proton radius now largest uncertainty in Lamb shift.
- Systematic error in normalization can affect radius.
- Variation of R with λ consistent with discrete ambiguity.
- Model-independent Sachs radius, ξ, consistent with Lamb shift.

Neutron Sachs Radius

$$\left\langle r^2 \right\rangle_n = -6\frac{dF_{1n}}{dQ^2} + \frac{3\kappa_n}{2m^2}$$

Dirac radius^2

Foldy term
-0.126 fm^2

- Atomic physics results cluster around two values differing by 5σ:
  - Oak Ridge: -0.115(3) fm^2
  - Dubna: -0.138(4) fm^2
- Alexandrov argues Dirac radius should be negative
- Others argue Foldy term cancelled, so that Sachs radius is negative. Accidental similarity between Foldy term and Sachs radius.

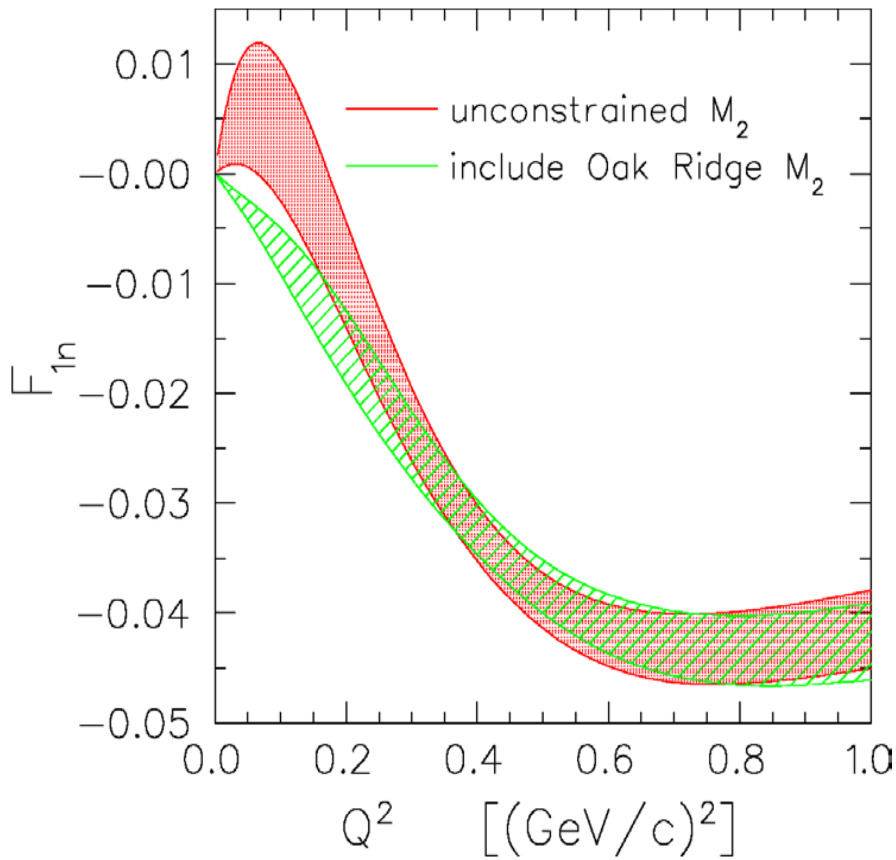

(e,e') data do not decide sign of Dirac radius

Extrapolation Scenarios for G_{En}

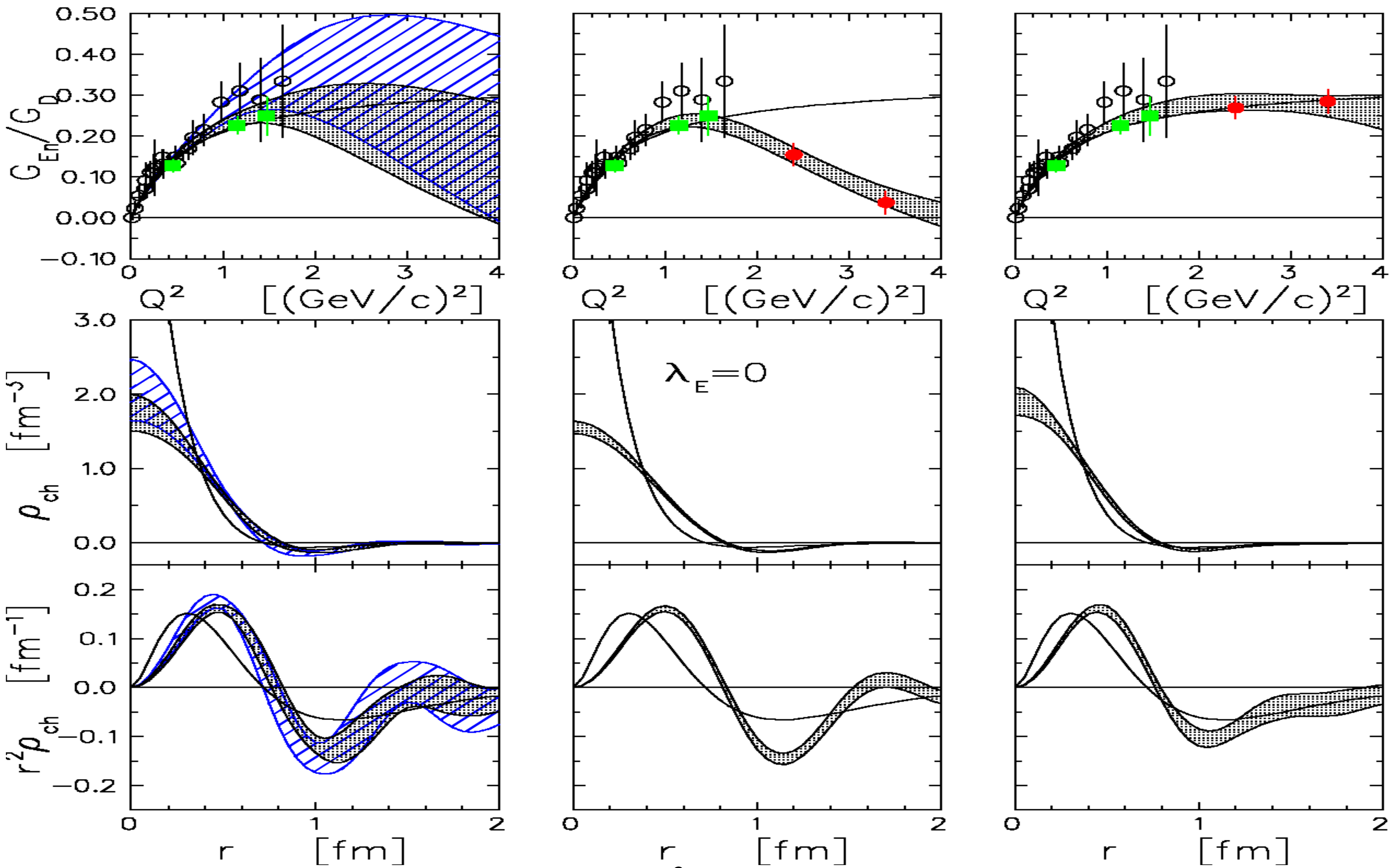

Proposed extension to larger Q^2 distinguishes between Galster extrapolation and more rapid decline favored by density model.

Conclusions

- Polarization techniques improve accuracy and higher Q^2 improves spatial resolution
  – new G_{Ep} data show proton charge broader than magnetization
  – new G_{En} data remain fairly consistent with Galster
- Linear expansion analysis
  – provides nearly model-independent fit to f.f. data
  – facilitates extrapolation and tests of scaling
- Relativistic inversion provides realistic radial densities
  – free of cusp at origin
  – charge densities suggest *u(r)* broader than *d(r)*
  – most considerations favor $\lambda_E = \lambda_M = 2$
  – proton charge radius consistent with QED
- Need reconciliation between Rosenbluth and polarization!

Future Prospects

- Approved experiment to extend G_{Ep} to 9 GeV^2 looking for sign change.
- Approved experiment to extend G_{En} to 3.4 GeV^2 will improve spatial resolution and challenge models.
- Need $Q^2 > 20\ GeV^2$ to reach scaling regime
- Technique can be applied to strange form factors from G0.
- Eagerly await lattice QCD calculations.